The role of *hindsight* in transcriptional regulation during *Drosophila melanogaster* development

by

Minhee Kim

A thesis
presented to the University of Waterloo
in fulfillment of the
thesis requirement for the degree of
Master of Science
in
Biology

Waterloo, Ontario, Canada, 2014

Declaration

I hereby declare that I am the sole author of this thesis. This is a true copy of the thesis, including any required final revisions, as accepted by my examiners.

I understand that my thesis may be made electronically available to the public.

Abstract

In *Drosophila melanogaster*, *hindsight* (*hnt*) encodes a putative Zinc-finger transcription factor that is expressed in a highly complex pattern during development. Despite an apparent wealth of information regarding the dynamic expression pattern of *hnt*, the cellular response and defined target genes of Hnt remain largely unknown. Hnt is important in various developmental processes, and recent work suggests that Hnt function is downstream of the Notch (N) signaling pathway. Interestingly, the mammalian homolog of *hnt* is *RAS-Responsive Element Binding Protein 1* (*RREB1*), which functions by binding to the RAS-responsive elements of the target gene promoters. Ras is a key downstream effector of the highly conserved Epidermal Growth Factor Receptor (EGFR) signaling pathway, yet the relationship between Hnt and EGFR signaling has not been extensively studied using the powerful approach of *Drosophila* genetics. This study involved a detailed examination of *hnt* mutant phenotypes and phenotypes associated with Hnt overexpression. Overall, this work revealed striking similarities between *egfr* and *hnt* mutant embryos. In particular, *hnt* mutant embryos were found to resemble *egfr* mutant embryos in their failure to properly develop peripheral nervous system (PNS) structures known as chordotonal organs and in their inability to recruit neighbouring secretory oenocytes. In addition, Hnt overexpression was found to induce ectopic DPax2 expression in an EGFR-dependent manner within the embryo. This relationship was also examined in a second developmental context, the pupal retinal neuroepithelium. Overall, the data presented suggests that Hnt's primary function in the development of the PNS is associated with potentiating EGFR signaling.

Acknowledgements

I would like to thank Dr. Bruce Reed for providing for me the opportunity to grow as a researcher under his guidance. I have received an incredible amount of support and knowledge working under his supervision, and I am truly grateful for all that I have gained through this experience. Over the years of doing research as an Undergraduate then as a Graduate student in the Reed lab, I have developed many valuable research skills that I will take with me on my future endeavors. I also want to thank my supervisory committee, Dr. Mungo Marsden and Dr. Moira Glerum for their continuous support and encouragement.

I would also like to thank both present and previous members of the Reed lab; Brittany Baechler, Yang Du, Elissa Downey, Samantha Widmeyer, Nicole Biro, and Janice Lee. Additionally, I would like to dedicate a special thank you to Dr. Dragana Miskovic for her exceptional guidance. Without her, none of this would have been possible. Thank you for believing in me and encouraging me to pursue research. I have developed a passion for Biology, particularly Developmental Biology, due to her guidance and I am truly grateful for this.

Finally, I would like to thank my friends and family who have been there for me during this process. I am so thankful for the amazing support I have from all those around me.

Table of Contents

List of Figures

List of Tables

List of Abbreviations

After Puparium Formation (APF)

Amnioserosa (AS)

Atonal (Ato)

CBF/Suppressor of Hairless/LAG-1 (CSL)

Chordotonal Organ Precursor (COP)

Cone Cell (CC)

Delta (Dl)

Discosoma Red Fluorescent Protein (dsRed)

Dorso-lateral Chordotonal Organ/Scolopodia (v'ch1)

Drosophila Pax2 (DPax2)

E26 Transformation-Specific (ETS)

Epidermal Growth Factor Receptor (EGFR)

Glass Mediated Response (GMR)

Green Fluorescent Protein (GFP)

Hindsight (Hnt)

Lateral Chordotonal Organs/Pentascolopodia (lch5)

Mastermind (Mam)

MicroRNA (miR)

Mitogen-Activated Protein Kinase (MAPK)

Notch (N)

Notch Extracellular Domain (N^{ECD})

Notch Intracellular Domain (N^{ICD})

Peripheral Nervous System (PNS)

Photoreceptor (R)

Primary Pigment Cell (1°)

Programmed Cell Death (PCD)

Proneural Cluster (PNC)

Pointed (Pnt)

Ras-Responsive Element Binding Protein 1 (RREB1)

Red Fluorescent Protein (RFP)

Rhomboid (Rho)

Secreted Spitz (sSpi)

Sensory Organ Precursor (SOP)

Secondary Pigment Cell (2°)

Shaven (sv)

Sparkling (spa)

Spitz (Spi)

Suppressor of Hairless (Su(H))

Tertiary Pigment Cell (3°)

Upstream Activating Sequence (UAS)

Ventral Chordotonal Organs (vch A,B)

Chapter 1: Introduction

1.1 Background

During development, conserved signaling pathways coordinate critical developmental responses such as cell proliferation, differentiation, and survival. Of particular interest are two signaling pathways that have been shown to repeatedly interact in a variety of contexts: the Notch (N) signaling pathway and the Epidermal Growth Factor Receptor (EGFR) signaling pathway (Lage and Jarman, 1999). These two pathways interact in a highly context-specific manner, where the cellular responses may differ depending on tissue-specificity, the level of expression, or target gene expression (reviewed in Sundaram, 2005).

1.1.1 Notch (N) Signaling Pathway

The canonical N signaling pathway is a conserved signaling pathway found throughout metazoan development. The Notch receptor is a transmembrane receptor consisting of an extracellular (N^{ECD}) and an intracellular domain (N^{ICD}). Activation of the Notch signaling pathway requires binding of its ligands, Delta or Serrate. Upon binding of the ligand, the Notch receptor is proteolytically cleaved. This causes separation of the two domains, and the cleaved N^{ICD} is released into the cell and directed into the nucleus. The N^{ICD} then interacts with CBF/Suppressor of Hairless/LAG-1 (CSL) family of transcription factors, such as Core Binding Factor 1/Suppressor of Hairless (Su(H)) and its co-activator Mastermind (Mam), ultimately directing target gene transcription (reviewed in Artavanis-Tsakonas et al., 1999).

The N signaling pathway mediates its functions primarily through two modes of action: inductive signaling and lateral inhibition (reviewed in Sundaram, 2005). During inductive signaling, one cell type signals to its neighboring cell through expression of a N ligand, activating the N response and ultimately influencing gene expression in the neighboring cell to promote a specific cellular response (Fig. 1.1A) (reviewed in Artavanis-Tsakonas et al., 1999). The process of lateral inhibition starts with a group of equivalent cells that are competent to acquire a certain fate. This process is reiteratively used during peripheral neurogenesis, and this equivalence group is designated as the proneural cluster (PNC). However, within the PNC, a single cell that acquires the highest level of proneural protein expression is selected as the sensory organ precursor (SOP). The SOP secretes high levels of the N ligand Dl, then laterally inhibits the surrounding cells within the PNC from acquiring a neural fate through the activation of the N signal, ultimately remanding these cells to an epidermal fate (Fig. 1.1B) (Cubas et al., 1991; de Celis et al., 1991; Jarman et al., 1995).

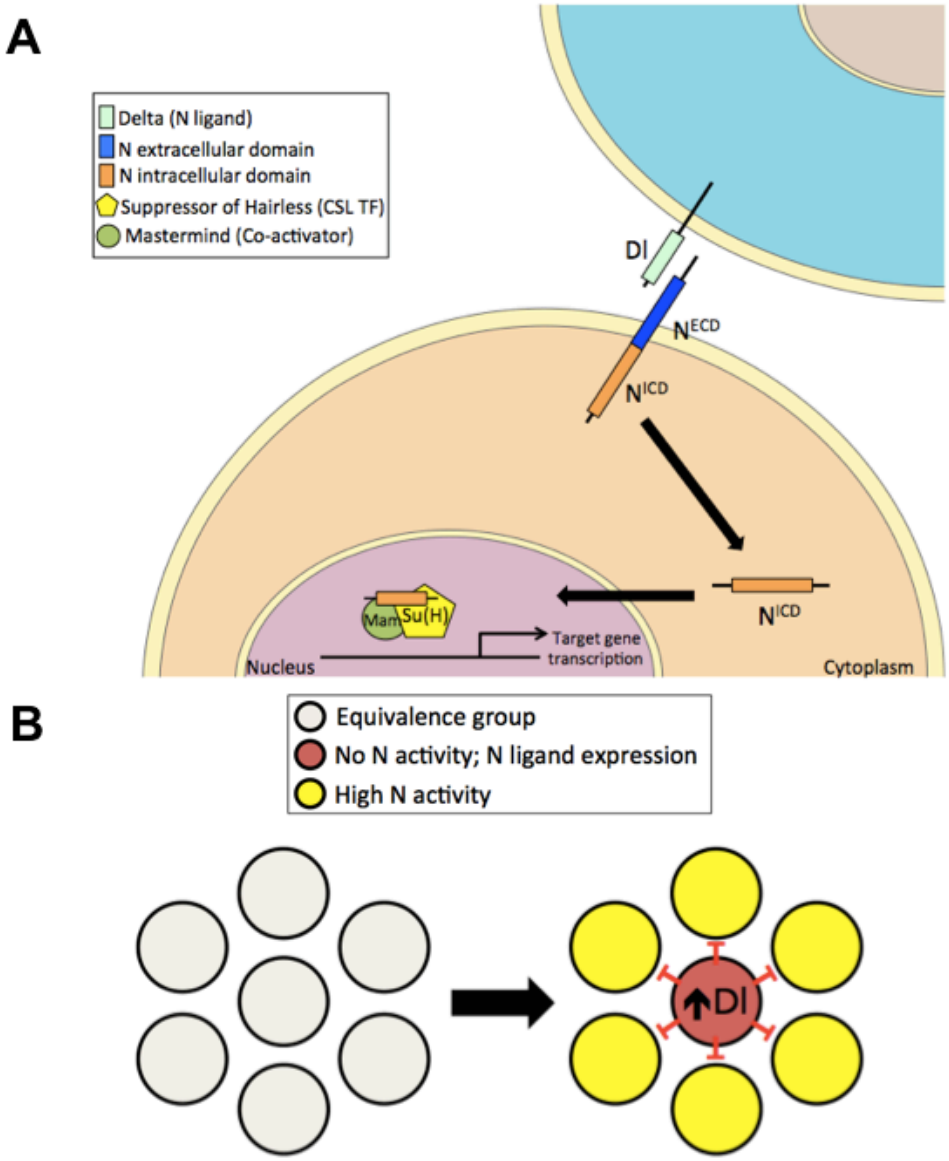

Figure 1.1 Inductive signaling and lateral inhibition by the N signaling pathway
(A) The activation of the N signaling pathway involves a bipartite N transmembrane receptor, consisting of the N extracellular domain (N^{ECD}) and intracellular domain (N^{ICD}). Binding of a N ligand, in this case Delta (Dl), results in proteolytic cleavage of the N transmembrane receptor, and subsequently the release of N^{ICD} into the cytoplasm. N^{ICD} is directed into the nucleus and affects target gene transcription through interaction with Supressor of Hairless (Su(H)) and Mastermind (Mam). Figure prepared using information provided by (Bray, 2006; Kopan and Ilagan, 2009)
(B) Lateral inhibition by N signaling starts with an equivalence group of cells, all capable of adapting to a certain fate (i.e. a neural fate). A single sensory organ precursor (SOP) is selected through feedback loops involving proneural genes in order to isolate the SOP (red), which will have no N activity but express and present the N ligand, Dl. The surrounding cells (yellow) will be receptive to the N signal through the ligand provided by the SOP, and ultimately, their fates will be remanded to an epidermal fate due to the activation of N. Figure prepared using information provided by (Bray, 2006)

1.1.2 Epidermal Growth Factor Receptor (EGFR) Signaling Pathway

In *Drosophila*, EGFR serves to activate the canonical Ras/Mitogen-Activated Protein Kinase (MAPK) pathway downstream of the receptor (Diaz-Benjumea and Hafen, 1994). The activation of EGFR requires the binding of one of its EGF ligands: Spitz, Keren, Gurken, and Vein (reviewed in Shilo, 2005). Spitz (Spi) is the most common ligand used to activate EGFR (Rutledge et al., 1992; Schweitzer et al., 1995), in comparison to the more restricted ligands, Keren, Gurken, and Vein, which have more spatially and temporally regulated expression patterns found throughout development. Prior to receptor binding, EGF ligands require intracellular cleavage by Rhomboid (Rho) and trafficking by Star, ultimately allowing for secretion of the active ligand. The secreted ligand is then able to bind to EGFR, activating the Ras/MAPK signaling pathway downstream of the receptor (reviewed in Shilo, 2005). The Ras/MAPK signaling pathway is responsible for phosphorylation of E26 transformation-specific (ETS) proteins, Pointed (Pnt) and Yan, ultimately affecting the transcription of the target genes (Gabay et al., 1996).

Pointed (Pnt) and Yan belong to the ETS-family of transcription factors. Both proteins are downstream effectors of MAPK phosphorylation to mediate target gene transcription. The *pnt* locus generates two isoforms of Pnt: PntP1 and PntP2. The PntP1 isoform acts as a constitutive transcriptional activator, while PntP2 activity is dependent on MAPK phosphorylation. Yan competes with Pnt for DNA-binding sites on target genes, and acts to repress transcription of target genes. The phosphorylation of Pnt via MAPK results in the increase of the transactivation of target genes, however, phosphorylation of Yan leads to the inhibition of its transcriptional repressive functions (Fig. 1.2) (Klämbt, 1993; O'Neill et al., 1994).

The EGFR signaling pathway has been implicated in various modes of differentiation, contact-dependent cell survival, and control of cell cycle progression (reviewed in Sundaram, 2005). Morphogenetic events such as dorsal closure of the amnioserosa (AS), maintenance of epithelial integrity of the trachea, photoreceptor (R) cell recruitment and differentiation in the eye, and development of the chordotonal organs and oenocytes require precise levels of input from EGFR signaling for proper development of the respective systems (Cela and Llimargas, 2006; Clifford and Schüpbach, 1992; Elstob et al., 2001; Freeman, 1996; Llimargas and Casanova, 1999).

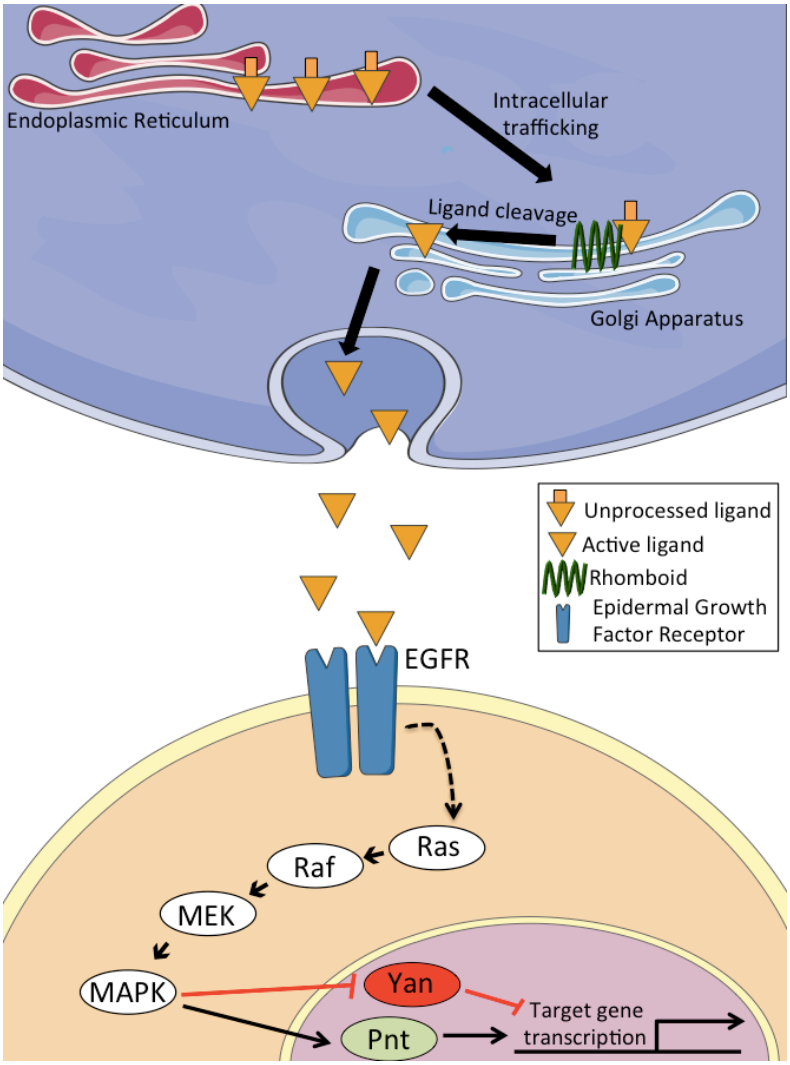

Figure 1.2 EGFR ligand processing and the activation of the EGFR signaling pathway
Prior to receptor binding, EGF ligands require cellular processing to become activated. The ligands undergo intracellular trafficking from the endoplasmic reticulum to the golgi apparatus to subsequently become cleaved by the golgi-associated protease, Rhomboid. The activated ligands are then secreted and bind to EGFR. Consequently, the activated EGFR dimerizes and is autophosphorylated, leading to the activation of the GTPase, Ras. Ras activation initiates a series of phosphorylation events through kinases downstream of Ras. Ultimately, once MAPK is phosphorylated, target gene transcription is affected through phosphorylation of the ETS-family of transcription factors, Yan or Pointed. Phosphorylation of Yan inhibits its transcriptional repressor function, thereby promoting target gene transcription. Phosphorylation of Pointed, a transcriptional activator, leads to higher activation of target gene transcription.
Figure prepared using information provided by (Shilo, 2005; Sundaram, 2005)

1.2 *Drosophila* Peripheral Neurogenesis

Peripheral neurogenesis throughout *Drosophila* development is a series of processes that are heavily reliant on the coordination between N and EGFR signaling pathways. The peripheral nervous system (PNS) consists of external mechanosensory organs, chemosensory organs, internal stretch receptors, and the visual system (Brewster and Bodmer, 1995; Carlson, 1996; Ready et al., 1976). All systems utilize lateral inhibition via N signaling for the general differentiation process of the SOPs, ultimately giving rise to one neuronal cell and other accessory cells that can be variable depending on the particular internal or external structure (reviewed in Lai and Orgogozo, 2004). Specifically, the development of embryonic internal stretch receptors known as chordotonal organs, as well as the process of photoreceptor differentiation in the developing retina show striking similarities involving the interactions between N and EGFR signaling pathways. In both systems, the selection of the SOPs requires expression of the proneural gene *atonal (ato)* (Jarman et al., 1995), *rho*, and *spi*. The expression of *ato*, a basic helix-loop-helix protein, in ectodermal cells allows these cells to acquire competencies to become neural precursor cells. In addition to *ato* expression, the selected SOP expresses high levels of *spi*, the unprocessed ligand of EGFR, and *rho*, which allows for proteolytic cleavage and activation of the ligand, ultimately activating the EGFR signal in neighboring cells for further cell recruitment and differentiation of both the photoreceptor cells and the chordotonal organs (Lage et al., 2004; Okabe and Okano, 1997).

1.2.1 *Drosophila* Embryonic Chordotonal Organ Development

During *Drosophila* embryogenesis, eight chordotonal organs arise in each abdominal hemisegment, consisting of a cluster of five lateral pentascolopodia, (lch5), one dorsolateral scolopodia (v'ch1), and two single ventral scolopodia (vchA, vchB) (Fig. 1.3). Each chordotonal organ (scolopodium) consists of one neuron, one ligament, one cap, and one sheath cell that are determined by lateral inhibition via N signaling (Brewster and Bodmer, 1995). Chordotonal organs are formed in two distinctive steps (Okabe and Okano, 1997). Initially, the founder cluster, consisting of five chordotonal organ precursors (COPs, C1-C5), arises from *atonal* expression and lateral inhibition. In the absence of *ato*, a complete absence of chordotonal organ formation is seen (Lage et al., 1997; Okabe and Okano, 1997), however, in the absence of *egfr*, only three scolopodia are seen due to the failure to recruit the remaining scolopodia (Elstob et al., 2001; Rusten et al., 2001). Expression of *ato, rho* and *spi* in COPs causes subsequent activation of the activated ligand, resulting in the completion of cell recruitment during chordotonal organ development. C1-C3 are three scolopodia from the lch5, where C2 and C3 will induce the remaining two scolopodia of the lch5. C4 is the vchB and C5 is the v'ch1, both of which contribute to the induction of vchA (Elstob et al., 2001; Lage et al., 1997; Okabe and Okano, 1997; Rusten et al., 2001).

During embryonic chordotonal organ development, non-neural secretory cells, oenocytes, are also recruited by the EGFR signaling pathway. Oenocytes are formed via delamination from the ectoderm upon receiving EGFR signals from dorsal-most COP of the lch5, the C1 (Elstob et al., 2001; Rusten et al., 2001). Each of the seven abdominal hemisegments that have clusters of approximately six oenocytes are in close proximity to

lch5 chordotonal organs (Hartenstein et al., 1992). Similar to the development of chordotonal organs, induction of oenocytes requires input from *ato*, *rho*, and *spi*. In the absence of any of the three inputs, a failure of oenocyte recruitment results. Excess signal can lead to induction of supernumerary oenocytes, indicating that proper oenocyte induction is sensitive to the levels of EGFR signaling (Elstob et al., 2001; Rusten et al., 2001). Overall, the presence of EGFR signaling is crucial for proper cell recruitment for both chordotonal organs and oenocytes (Elstob et al., 2001; Lage et al., 1997; Lage et al., 2004; Okabe and Okano, 1997; Rusten et al., 2001). This mode of cell recruitment and differentiation is highly analogous to photoreceptor development in the retina (Freeman, 1996; Okabe and Okano, 1997).

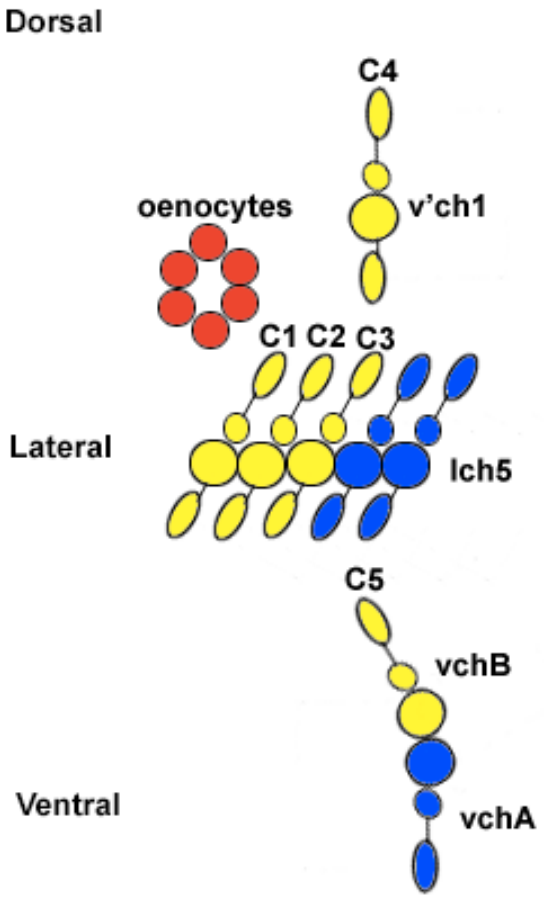

Figure 1.3 Schematic of the embryonic chordotonal organs and oenocytes
Each abdominal hemisegment consists of eight chordotonal organs: one located dorso-laterally (v'ch1), five located laterally (lch5), and two in the ventral region (vchA, vchB). The recruitment and development of the chordotonal organs depends on the chordotonal precursor cells (C1-C5, yellow) expressing adequate levels of *atonal*, *rhomboid*, and *spi*. The secretion of activated ligands from C1-C5 activates EGFR signaling to further recruit the remaining three chordotonal organs (two of the lch5 and vchA, blue) and permits the recruitment of non-neural oenocytes (red). Figure adapted from (Gould et al., 2001)

1.2.2 Drosophila Retinal Development

The *Drosophila* compound eye is composed of approximately 750 individual photoreceptor units called ommatidia. In *Drosophila*, the development of the ommatidia is a popular paradigm for studying cellular recruitment, differentiation, death, and interactions between cell signaling pathways (Ready et al., 1976; Wolff and Ready, 1991). The recruitment of cells for an ommatidial cluster undergoes a stereotypical sequence of events and induction patterns, consisting of intricate interplay between various signaling pathways. Each ommatidium is comprised of eight neuronal photoreceptor (R) cells (R1-R8), four cone cells (CCs), and two primary pigment cells (1°). All of the individual units of ommatidia share surrounding lattice cells in the finalized hexagonal lattice, comprised of two types of pigment cells (2°/3°) and interommatidial bristles (Ready et al., 1976). Initially, the neuronal cells (R cells) are specified, and the founder cell R8 is isolated from a proneural cluster via N-dependent lateral inhibition. As mentioned above, similar to the chordotonal organs, the selection of R8 is dependent on levels of *ato* expression (Lage et al., 1997; Okabe and Okano, 1997; Yang and Baker, 2001). Following R8 specification, the R2/R5 and R3/4 cells are recruited, forming a 5-cell cluster. Subsequently, R1/R6/R7 cells are recruited, followed by recruitment of cone cells and lastly the accessory pigment cells (Ready et al., 1976).

With respect to developmental timing, specification of all R cells and CCs occurs during larval stages. The recruitment of accessory cells occurs after puparium formation (APF) and after eye disc eversion (Fig. 1.4), and is highly dependent on levels of EGFR signaling and N signaling to control cell survival and cell death at appropriate time points to achieve the highly organized retina structure (Miller and Cagan, 1998). EGFR

signaling is used reiteratively throughout retinal morphogenesis during the differentiation and recruitment of all cell types. In the developing larval eye disc, *egfr* is not required for the establishment of the founder R8 cell, but is required for subsequent R cell recruitment. When excess EGFR signaling is activated, supernumerary R cell recruitment is seen (Domínguez et al., 1998). Therefore, it is critical for the EGFR signal to be activated and inhibited within specific time frames to achieve successive waves of recruitment of different cell types (Freeman, 1996).

During the final stages of eye morphogenesis, programmed cell death (PCD) is required in the undifferentiated cells surrounding the ommatidia (secondary and tertiary pigment cells). A wildtype apical surface of the ommatidium consists of four CCs and two 1°s that are encased by twelve lattice cells: three bristle cells, six 2°s, and three 3°s. PCD occurs in the lattice cells between 18-40 hr APF, eliminating approximately 2000 excess undifferentiated cells present within the lattice, and ultimately forms twelve lattice cells shared by each ommaditium (Cagan and Ready, 1989). During this time, excess Ras signal promotes cell survival while excess N signal can promote cell death (Miller and Cagan, 1998). The formation of interommatidial bristles also undergo the stereotypical lateral inhibition process, however, the specific mechanism regarding the formation of interommatidial bristles is largely unknown.

Numerous genes are involved in the development of embryonic chordotonal organs and the retina. Of interest is the *hindsight* (*hnt*) gene that is strongly expressed throughout peripheral neurogenesis. Robust expression of Hnt is seen throughout embryonic chordotonal development and retinal development within the PNS lineage. However, the regulation of *hnt* in these contexts is unknown. Interestingly, recent

research from our lab suggests a role of Hnt to mediate both N and EGFR signaling pathways in the context of the development and maintenance of the adult midgut (Baechler, 2014). In support of many publications presenting *hnt* as a N-responsive gene in several different contexts (Housden et al., 2013; Krejci et al., 2009; Sun and Deng, 2007; Terriente-Felix et al., 2013), in the adult midgut, Hnt was shown to act downstream of N signaling. In addition, the maintenance of Hnt expression was shown to be dependent on the EGFR signaling (Baechler, 2014). Since N and EGFR signaling are providers of critical inputs during peripheral neurogenesis, the responsiveness of *hnt*, as well as its potential role during these processes, requires further investigation.

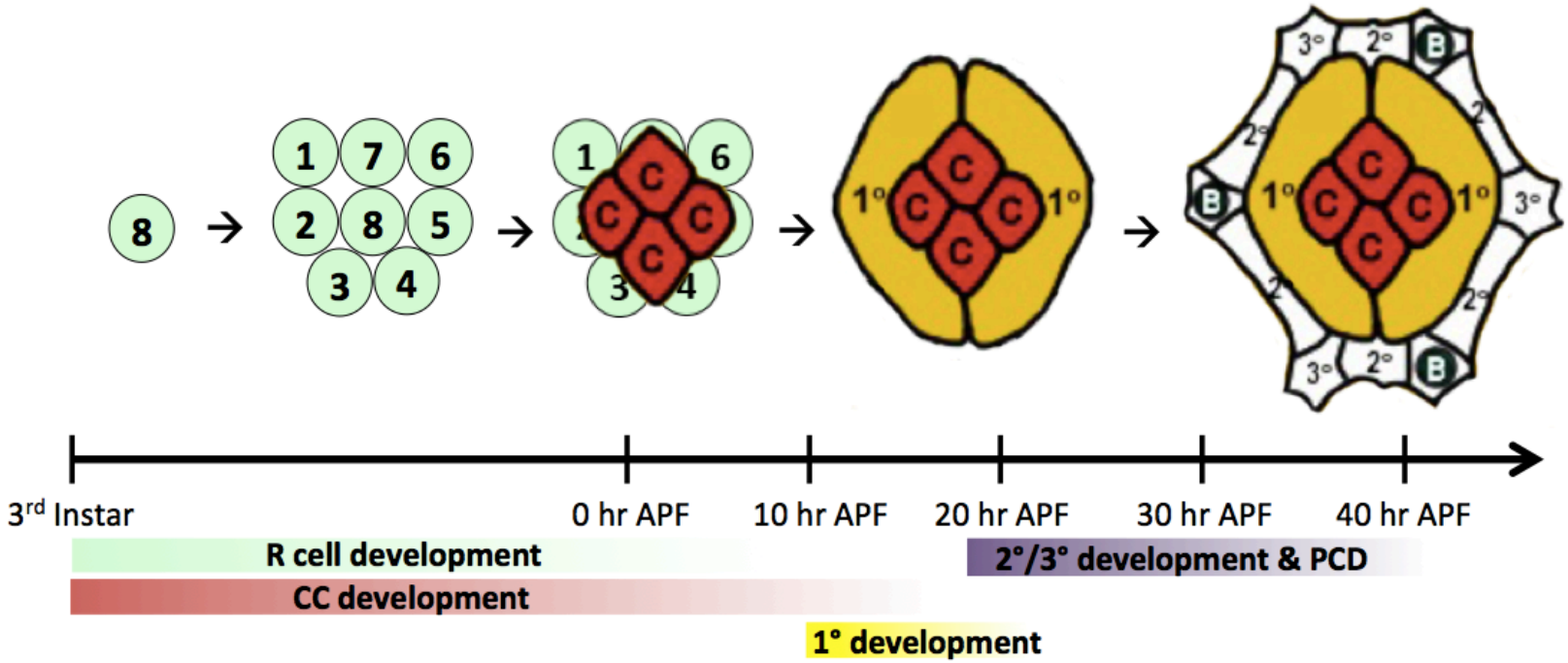

Figure 1.4 *Drosophila* ommatidial development
Eye morphogenesis begins at third instar larval stage. At this stage, the photoreceptor cells (R cells) are selected and recruited using lateral inhibition via N signaling and inputs from the EGFR signaling pathway. R8, the founder cell, is responsible for the recruitment of R1-R7 through the secretion of activated EGF ligands. Subsequently, CCs are induced by inputs from the R cells. In the pupal stages, the development of all pigment cells (1°/2°/3°) and bristle cells occurs, followed by PCD, which removes undifferentiated cells to ultimately form a hexagonal array of ommatidia. Each ommatidium is comprised of eight R cells, four CCs, and two 1°s, which are surrounded by the shared lattice cells, consisting of 2°s and 3°s and interommatidial bristles. Figure prepared using information provided by (Freeman, 1996; Voas and Rebay, 2003)

1.3 Hindsight (Hnt)

The *hindsight* (*hnt*) (Flybase – *pebbled (peb)*) gene of *Drosophila melanogaster* encodes a protein containing 14 C_2H_2-type zinc finger protein with a highly complex expression pattern found throughout *Drosophila* development. Two independent studies of sensory organ development identified *hnt* as a gene that is significantly upregulated in specified SOPs (Bufflin and Gho, 2010; Reeves and Posakony, 2005). However, the regulation of *hnt* expression and its function in the SOP cells has not been well characterized thus far. Previous research suggests the significance of Hnt as being a critical factor for numerous developmental processes. Mutations to *hnt* display embryonic lethality, and therefore *hnt* was classified as an essential gene required for proper *Drosophila* embryonic morphogenesis. In this context, *hnt* is required for the maintenance of the amnioserosa (AS), an extraembryonic membrane composed of squamous epithelial cells. In addition, Hnt is an essential factor involved in the permissive control of germ band retraction, where *hnt* mutant embryos display an unretracted germ band phenotype (Yip et al., 1997). Moreover, *hnt* mutants are unable to proceed with tracheal morphogenesis due to the loss of epithelial integrity in developing tracheal cells (Wilk et al., 2000). Following embryonic development, Hnt promotes the differentiation of crystal cells within the hemocyte lineage (Terriente-Felix et al., 2013). Furthermore, Hnt is a regulator of the mitotic cycle to endocycle (M/E) transition in *Drosophila* follicle cells in the adult ovary. Hnt is also required during several stages of retinal development, in addition to neuronal morphogenesis in adult flies (Oliva and Sierralta, 2010; Pickup et al., 2002; Sun and Deng, 2007).

Throughout *Drosophila* development, the expression of Hnt can be found in tissues such as the AS, trachea, components of the PNS, the developing midgut, follicular cells in the ovary, cells of the hemocyte lineage, as well as cells during retinal development (Lamka and Lipshitz, 1999; Pickup et al., 2002; Sun and Deng, 2007; Terriente-Felix et al., 2013; Wilk et al., 2000; Yip et al., 1997). While the general functions associated with Hnt have been broadly studied, specific molecular functions of Hnt, as well as the mechanism that controls *hnt* expression remain elusive. In several contexts such as *Drosophila* muscle cell lines, hemocyte-like cell lines, and ovarian follicle cells, *hnt* has been identified as a N-responsive gene (Housden et al., 2013; Krejci et al., 2009; Sun and Deng, 2007; Terriente-Felix et al., 2013). However, in the developing retina, Hnt acts upstream of N signaling to modulate levels of the N ligand, Dl (Pickup et al., 2009). Despite the numerous ties between N signaling and *hnt* expression in *Drosophila*, the human homolog of *hnt*, Ras-Responsive Element Binding Protein 1 (RREB1), is a downstream effector of the canonical Ras/MAPK signaling pathway (Zhang et al., 1999). Since the regulation of embryonic Hnt expression is largely unknown, it is of interest to determine the responsiveness and function of *hnt* to conserved signaling pathways such as N and EGFR signaling pathways.

1.4 Ras Responsive Element Binding Protein 1 (RREB1)

The mammalian homolog of *hnt*, *RREB1*, encodes a Zinc-finger transcription factor (Thiagalingam et al., 1997; Zhang et al., 1999). RREB1 binds to Ras-responsive elements, ultimately regulating the transcriptional outputs of the Ras/MAPK signaling pathway. RREB1 has multiple roles to regulate gene expression. It has been well established that RREB1 can act as either a transcriptional repressor to attenuate target gene expression, or as a transcriptional activator to potentiate target gene expression. RREB1 directly binds to regulatory regions of genes such as *calcitonin* and *p53* to upregulate the expression of the respective genes (Liu et al., 2009; Thiagalingam et al., 1997). However, its activity as a transcriptional repressor has been found to downregulate genes such as *hZIP1* and $p16^{INK4a}$ (Milon et al., 2010; Zhang et al., 2003). Additionally, RREB1 directly binds and represses *microRNA* (*miR*)-*143* and *miR*-145, inhibitors of Ras signaling, ultimately enabling higher levels of the Ras signal (Kent et al., 2010).

Although Hnt remains to be a putative transcription factor, its zinc-finger domains and consistent nuclear localization suggest that it is indeed a transcription factor (Yip et al., 1997). In addition, Hnt binds to similar DNA sequences and carries similar functions using the same domains as the DNA-binding domain as RREB1, indicating high functional conservation for the two proteins. Furthermore, expression of RREB1 in the AS of *hnt* mutant embryos that display failure in germ band retraction was shown to rescue this mutant phenotype, indicating a functional overlap of the two proteins (Ming et al., 2014). Therefore, since RREB1 has been implicated in multiple forms of tumors and cancer, investigating the regulation of and functions associated with *RREB1* by using the *Drosophila* model of *RREB1* homolog, *hnt*, is of significance.

1.5 *Drosophila* Pax2 (DPax2): A potential transcriptional target of Hnt

A recent microarray analysis performed in our lab of the transcriptional profiles of embryos ubiquitously overexpressing Hnt identified DPax2 as a putative transcriptional target of Hnt. The microarray result was confirmed by in-situ hybridization and immunostaining, and established that Hnt overexpression induces ectopic DPax2 expression, suggesting a possible regulatory relationship between the two genes (Du, 2013).

1.5.1 DPax2

DPax2 encodes a paired-domain transcription factor, homologous to the vertebrate *Pax2* gene. DPax2 is primarily involved in the development of CCs of the eye and the adult sensory organ, bristles. There are two main allelic forms of *DPax2*, *sparkling* (*spa*) and *shaven* (*sv*), driving the eye-specific expression of DPax2 and the sensory organ-specific expression in the adult fly, respectively. The transcriptional regulation of *DPax2* is highly complex during *Drosophila* development. During embryogenesis, *DPax2* expression is seen within the developing components of the PNS and the central nervous system (Fu et al., 1998). The regulation of embryonic *DPax2* expression is not well characterized, however, the expression of *DPax2* pertinent to the two identified allelic forms, *spa* and *sv*, have been well characterized in later stages during *Drosophila* morphogenesis. The *spa* enhancer is a 362 bp region located within the fourth intron of the *DPax2* gene and serves to specifically activate *DPax2* in the developing eye (Fu and Noll, 1997). The *sv* enhancer is a 6.7 kb region upstream of the *DPax2* gene, including a portion of the 5' untranslated region, and activates *DPax2* expression only within the developing SOPs (Kavaler et al., 1999).

1.5.2 A Model for Cone Cell Induction

The *spa* enhancer allows CC-specific expression of DPax2 and has been extensively studied to date. A combinatorial model of activation of *DPax2* expression of the *spa* enhancer has been identified, and this model suggests the requirement of a tripartite input system: the nuclear effector of the N signaling pathway, Su(H), the nuclear effectors of the EGFR signaling pathway, ETS proteins Yan and Pnt, and Lozenge, the *Drosophila* homolog of the Runt-domain family of transcription factors (Flores et al., 2000). Within the *spa* enhancer, 5 binding sites for Su(H), 4 binding sites for ETS proteins, and 3 binding sites for the Lozenge/Runt domain are present (Flores et al., 2000; Swanson et al., 2010). The 3 inputs are necessary for the transcriptional activation of *DPax2* in the developing CCs. The removal of each input results in the loss of DPax2 expression in CC precursors of the developing larval eye discs (Flores et al., 2000). Interestingly, it has been shown that Hnt and DPax2 have an indirect relationship during CC induction (Pickup et al., 2009). According to Pickup and others (2009), Hnt is able to regulate DPax2 expression indirectly by modulating levels of the N ligand, Dl.

To determine the mechanism of ectopic DPax2 induction through Hnt overexpression in the embryo, this combinatorial model for CC induction was extrapolated to test for a potential indirect mode of activation of DPax2 through Hnt overexpression, in addition to testing whether a direct correlation was present between the expression of Hnt and DPax2.

1.6 Research Goals and Objectives

Given that the present information regarding Hnt is primarily pertinent to its role in the regulation of morphogenesis, I wished to investigate how Hnt expression is regulated in the developing embryo by testing to see whether *hnt* is dependent on, and/or is responsive to inputs from either N or EGFR signaling. Moreover, in continuation of the work started by a former graduate student in our lab, the relationship of Hnt and DPax2 was investigated to elucidate a mechanism that leads to ectopic DPax2 induction upon overexpression of Hnt.

Chapter 2: Materials and Methods

2.1 Fly Genetics

All fly stocks were stored and maintained at 25°C on standard yeast and molasses-based media unless stated otherwise. Stocks used during GAL80$^{temperature\ sensitive}$ (GAL80^{ts}) experiments were stored at 18°C then shifted to 29°C. For information regarding list of stocks used and crossing schemes, see Appendix A.

2.2 GAL4-UAS System

The GAL4-UAS system utilizes the yeast transcriptional activator, GAL4, to bind to and activate the expression of genes under the control of the responding element, the Upstream Activating Sequence (UAS). In *Drosophila*, this system is used as an inducible gene expression system to manipulate expression of a gene of interest under the control of a particular promoter. The expression of the GAL4 protein is controlled by a specific promoter, to allow for precise spatial and temporal control of the desired gene expression. The GAL4 protein can bind to particular regions of DNA that contain the responder UAS sites, with each UAS site being comprised of 17 basepairs. The responding UAS element is attached with the gene of interest, and transcription of the gene of interest is dependent on the presence of the GAL4 driver.

For the purposes of gene misexpression in *Drosophila*, this system is a bipartite system where the GAL4 driver and the UAS responder remain separate until parental lines are crossed together. Once the parental lines are crossed, resulting in progeny that carry both the GAL4 and UAS constructs together will activate the expression of the gene of interest under the control of a specific promoter (Fig. 2.1A) (reviewed in Duffy, 2002).

2.3 GAL80 temperature sensitive (ts)

To allow for higher degree of control and inducibility of the desired gene expression, an additional element, GAL80, which specifically binds to and inhibits transcriptional activity of the GAL4 was used (reviewed in Duffy, 2002). In *Drosophila*, the GAL80 protein is modified to allow for temperature-dependent repression and activation of the GAL4 transcriptional activity. The modified $GAL80^{ts}$ protein contains conditionally active inteins alleles, which are protein introns, from the *VMA1* gene. The inserted inteins require post-translational splicing, which is temperature dependent, to temporally regulate the activity of the $GAL80^{ts}$. At the permissive temperature, 18°C, splicing of the inteins allow production of functional GAL80, prohibiting transgene expression through the GAL4-UAS system. However, at the non-permissive temperature, 29°C, the splicing of the inteins cannot occur, thus producing a non-functional GAL80, resulting in expression of the transgene through the GAL4-UAS system. In addition, $GAL80^{ts}$ reversibly functions upon shifting to and from permissive temperatures and non-permissive temperatures (Fig. 2.1B) (Zeidler et al., 2004).

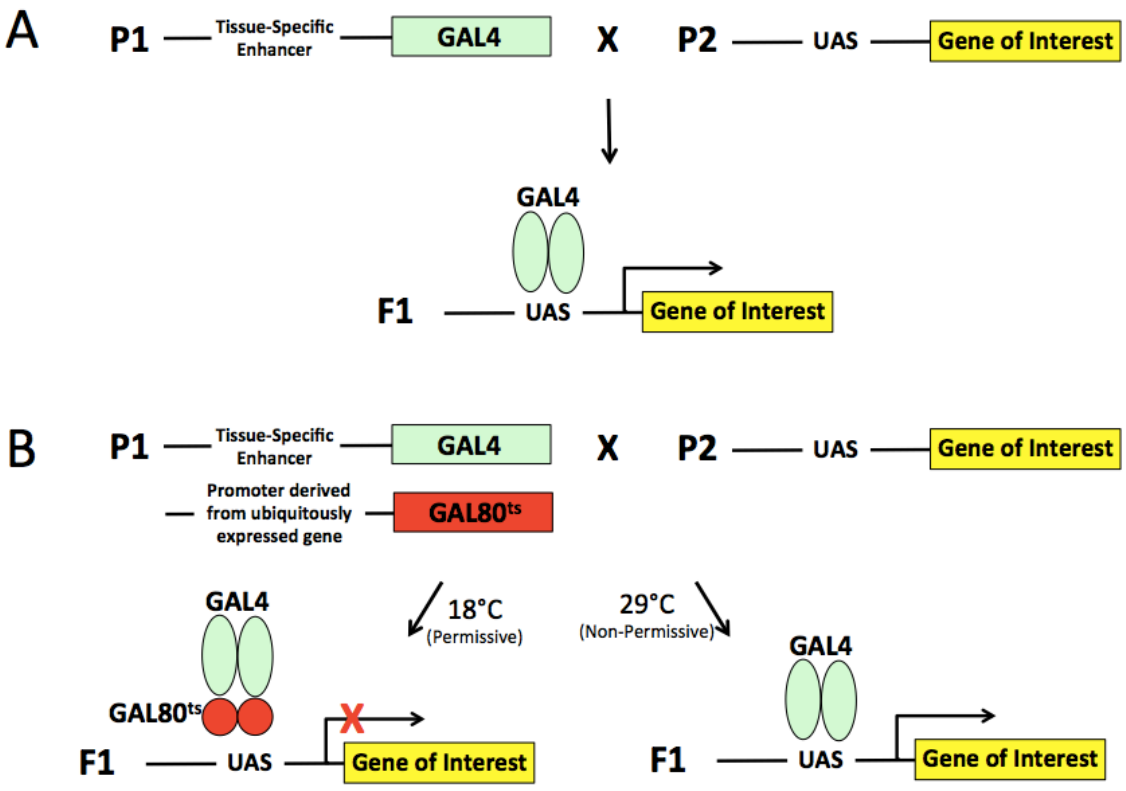

Figure 2.1 The GAL4-UAS system of inducible gene expression
(A) In *Drosophila*, expression of any desired transgene can be directed using the bipartite GAL4-UAS system. The system utilizes two yeast-derived constructs, the GAL4 transcriptional activator and the UAS responder. Parent (P) 1 carries a tissue-specific genomic enhancer upstream of the GAL4 coding sequence, which temporally and spatially regulates GAL4 protein expression. When P1 is crossed with P2, which carries the gene of interest downstream of UAS, the resulting progeny (F1) produce GAL4, which subsequently binds to the UAS-gene of interest, ultimately activating tissue-specific transcription of the gene of interest. (B) For more stringent temporal control of the GAL4-UAS system, $GAL80^{ts}$ is used to conditionally direct expression of the gene of interest. $GAL80^{ts}$ is downstream of a promoter derived from an ubiquitously expressed gene, such as tubulin. P1 and P2 carrying GAL4, $GAL80^{ts}$, and UAS-gene of interest constructs are crossed and the resulting progeny inherits all three constructs. At permissive temperatures (18°C), the production of functional $GAL80^{ts}$ represses GAL4 activity, ultimately inhibiting target gene transcription. At non-permissive temperatures (29°C), $GAL80^{ts}$ is non-functional, allowing GAL4 to bind to the UAS responder to activate desired gene expression.

2.4 Embryo Dechorination and Fixation

Embryos were collected following an overnight mating set-up of the desired parental genotypes. All embryos subjected to immunostaining or live-imaging were dechorionated prior to following respective protocols (see Section 2.5 and 2.8). Dechorionation is a process of removing the outer protective layer, the chorion, of the embryo. Two methods were utilized depending on the quantity of the embryos that were collected. If large amounts of embryos were collected, a mild bleach mixture consisting of 50% bleach, 40% dH_2O, and 10% 1XPBT (0.1% Triton X in 1X phosphate buffered saline (PBS)) was used to soak the embryos for 3-4 minutes (min). The embryos were drained using a small piece of cheesecloth then thoroughly washed with dH_2O. However, if only a small quantity of collected embryos were available, embryos were individually dechorionated using forceps to remove the chorion layer by gently rolling the embryo on a double-sided tape attached to a slide. Proceeding dechorionation of the embryos, embryos were subjected to a fixation process in 5 ml of 3.7% formaldehyde in 1XPBS and 5 ml of methanol for 20 min.

2.5 Pupal Retina Dissection and Fixation

White prepupae were collected and aged for 48 hours (hr) at 25°C. For experiments involving GAL80^{ts}, white prepupae were collected then aged for 24 hr at 18°C, then transferred to 29°C for an additional 24 hr. On a slide with double-sided tape, the 48 hr APF pupae were then carefully placed to remove the pupal case. Next, the dissected pupae were placed into 1XPBS in a small dissecting dish using a brush, then gently pushed down to the bottom of the dish to break the surface tension. Holding a pupa laterally with one forcep by grabbing the abdomen area, the proboscis was pulled with another forcep to open up the head of the pupa. Once the retina that is attached to the optic lobe was found, it was transferred into a new dissecting dish containing fresh 1XPBS by using a P200 micropipette. This process was repeated until a desired amount of retinas attached to the optic lobe were dissected.

The dissected retinas were then transferred to an eppendorf tube and once the 1XPBS was removed, 500 μl of 3.7 % formaldehyde in 1XPBS was added and fixed on the shaker for 20 min.

2.6 Immunostaining

Prepared embryos were rehydrated with increasing concentrations of 1X PBS in methanol (prepared retinas did not require rehydration) and then washed 3 times in 1X PBT for 10 min per wash. Using 1% normal goat serum, 5% BSA, and 1X PBT, the prepared embryos or pupal retinas were blocked to prevent non-specific binding of the primary antibody for 1 hr at room temperature. Then, the primary antibody was added into 1% normal goat serum, 5% BSA, and 1X PBT according to proper dilutions for respective antibodies (listed below), then incubated overnight at 5°C. The diluted primary antibody was removed, and then saved for up to 3 more uses. Subsequently, the embryos or retinas were washed 3 times with 5% BSA and 1X PBT in a 1:1 ratio for 15 minutes per wash. An additional blocking step followed to prevent non-specific binding of the secondary antibody using normal goat serum, 5% BSA, and 1X PBT, and was incubated for 1 hr at room temperature. After blocking, appropriate amount of the secondary antibody was added to normal goat serum, 5% BSA, and 1X PBT and incubated for 2 hours at room temperature covered in foil. Then, the secondary antibody was removed, followed by 4 washes with 1X PBT for 15 min per wash, then a gravity wash with 1X PBS. The stained embryos or retinas were then subjected to a glycerol series with increasing concentrations of glycerol and decreasing concentration of 1X PBS. Finally, the embryos or retina were put in DABCO, a mounting solution, ready to be placed on a microscope slide for imaging purposes.

The dilutions for primary antibody stains were as follows: mouse monoclonal anti-Hindsight antibody (1:25; Howard Lipshitz, University of Toronto), mouse monoclonal anti-22C10 antibody (1:500; Developmental Studies Hybridoma Bank

(DSHB)), mouse monoclonal anti-Cut antibody (1:20; DSHB), mouse monoclonal anti-Armadillo antibody (1:100; DSHB), rabbit monoclonal anti-Croquemort antibody (1:1000; Nathalie Franc, Scripps Research Institute), and rabbit monoclonal anti-DPax2 antibody (1:2000; Joshua Kavaler, Colby College). The secondary antibodies used were: Alexa Flour® 488 goat anti-mouse and goat anti-rabbit (1:500; Cedarlane Labs), and TRITC goat anti-mouse (1:500; Cedarlane Labs).

2.7 Live-imaging of embryos and pupae

Embryos and pupae expressing green fluorescent protein (GFP) or discosoma red fluorescent protein (dsRed) reporters were dechorionated and removed from the pupal cases, respectively, on a double-sided tape prior to live imaging. Using the hanging drop technique (Reed et al., 2009) to prevent compression of the embryos or pupae, time-lapse confocal microcopy was performed using a Nikon Eclipse 90i microscope.

2.8 Laser Confocal Microscopy

All stained embryos or pupal retina as well as those prepared for live imaging were imaged using a Nikon Eclipse 90i microscope fitted with a Nikon D-eclipse C1 scan head using the Nikon EZ-C1 software at 20X objective. All images were processed through the Nikon EZ-C1 software, NIH ImageJ software, and Adobe Photoshop.

Chapter 3: Results

3.1 Tissue-specificity of Hnt expression in response to N signaling

It has been previously established that *hnt* interacts with and responds to N signaling in a variety of contexts. For example, it has been proposed that Hnt is required for the increased expression of the N ligand, Dl, during CC induction in the pupal retina (Pickup et al., 2009). Additionally, *hnt* has been identified as a direct target gene of N in the developing pupal muscle, larval lymph gland, and adult follicular epithelium (Housden et al., 2013; Krejci et al., 2009; Sun and Deng, 2007; Terriente-Felix et al., 2013). The regulation of *hnt* expression in the developing embryo is not well characterized, and therefore my first line of investigation was to ask if *hnt* expression is dependent on N signaling during embryogenesis.

3.1.1 Embryonic Hnt expression is selectively responsive to N

In order to examine the effect of N signaling on *hnt* expression, a mutant allele of *N*, N^{55e11}, and the GAL4-UAS system were utilized (see Materials and Methods) for the analysis of *N* loss of function and activation, respectively. To activate N signaling, a cleaved form of the N transmembrane receptor, *UAS-*N^{intra}, was used. In both *N* loss of function and activation, embryonic Hnt expression was examined via immunostaining. Examination of the Hnt expression pattern in N^{55e11} embryos revealed expression of HNT in the AS and throughout the hypertrophic PNS that is a well-known characteristic of *N* mutants (Fig. 3.1C). The hypertrophic PNS of *N* mutants, which is frequently referred to as a neurogenic phenotype (de Celis et al., 1991), is readily visualized using anti-22C10, a marker for differentiated neurons. Compared to the wildtype expression of both Hnt and

22C10 (Fig. 3.1A, B, respectively), in embryos overexpressing activated N, the areas of Hnt-positive cells are strikingly similar to the expanded neuronal populations, suggesting that neuronal Hnt expression in the developing PNS is independent of N signaling (compare Fig. 3.1C and 3.1D).

Overexpression of *UAS-N^{intra}* universally in embryos using the *daughterless-GAL4* (*daGAL4*) driver resulted in a dramatically different Hnt expression pattern and a failure in the process of germ band retraction (Fig. 3.1E). The expression of Hnt, in this context, was confined to what appears to be the tracheal placodes and unknown scattered cells in the anterior region of the embryo. These embryos also showed a striking absence of Hnt expression in the PNS. However, universal activation of N is well known to eliminate neuronal differentiation (reviewed in Louvi and Artavanis-Tsakonas, 2006). Therefore, the lack of anti-Hnt staining was presumably due to the absence of PNS development in this background. To confirm that Hnt expression in the developing trachea persists in the context of global activation of N signaling, a deficiency, *Df(1)rb^{1}*, which is known to be associated with the absence of Hnt expression in the developing trachea (Wilk et al., 2000), was crossed to recover embryos overexpressing *UAS-N^{intra}* in this deficiency background. In the *Df(1)rb^{1}* embryos overexpressing *UAS-N^{intra}*, the presumed tracheal expression of Hnt was abolished, confirming that this expression was indeed tracheal. However, the unknown Hnt-expressing cells located in the anterior region of the embryo persisted, indicating that these cells were not of tracheal origin (Fig. 3.1F)

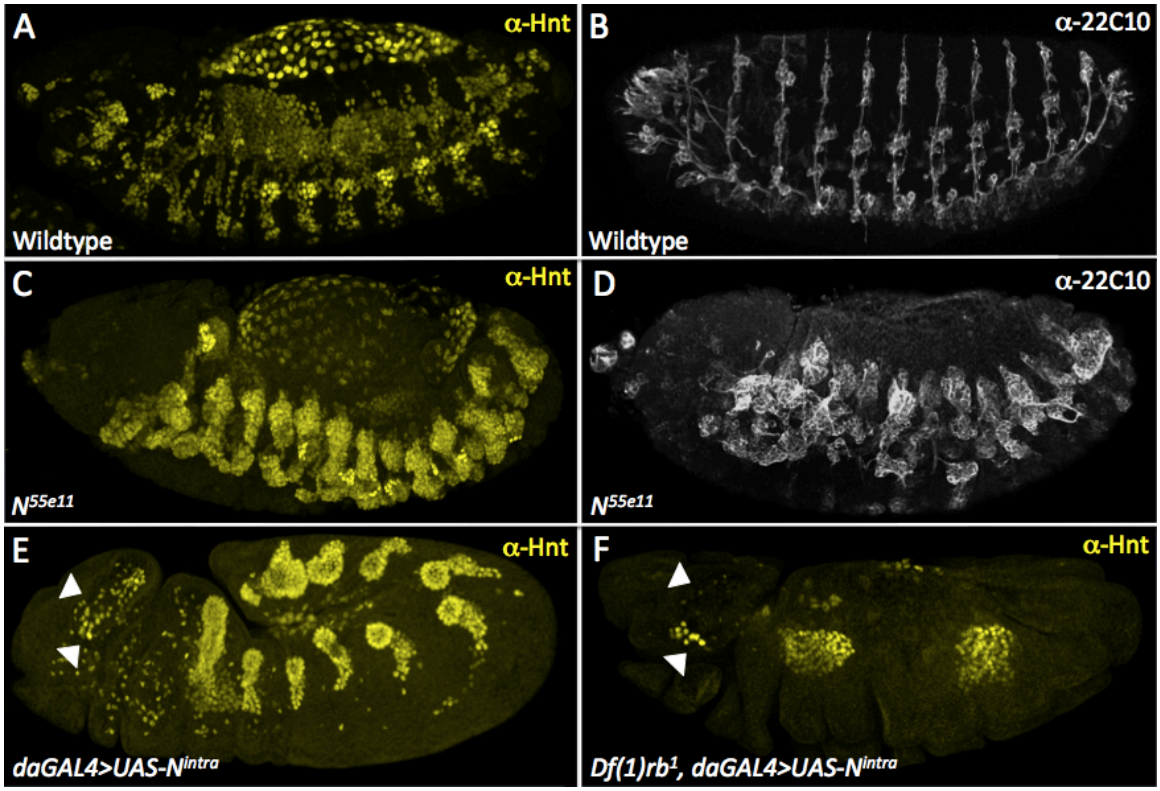

Figure 3.1 Tissue-specific responsiveness of embryonic Hnt expression to N signaling
Endogenous Hnt expression and outlines of differentiated neurons were detected by anti-Hnt (yellow) and anti-22C10 (white), respectively. Wildtype expression of Hnt (A) and neurons (B) compared to N^{55e11} embryos (C, D). Hnt expression (C) is observed throughout the stereotypical hypertrophic PNS phenotype observed in *N* mutants (D). Overexpression of activated N (*daGAL4>UAS-*N^{intra}) leads to Hnt-positive cells in the anterior region of the embryo (E, white arrowheads) as well as presumed tracheal placodes. The absence of tracheal-specific expression of Hnt in $Df(1)rb^{1}$ embryos overexpressing activated N results in the elimination of Hnt expression in the presumed tracheal placodes. However, the Hnt-positive scattered anterior cells persist (F, white arrowheads) in addition to the normal expression of Hnt in anterior and posterior midgut.

3.1.2 Embryonic overexpression of activated N induces hemocyte-like cells expressing Hnt

In embryos associated with global activation of N signaling, Hnt-positive cells were observed scattered throughout the anterior region. As outlined in the previous section (Section 3.1.1), these cells were neither neuronal nor tracheal. As mentioned in Chapter 1, previous findings suggest that *hnt* is responsive to N in some cell types, including the hemocyte lineage and the muscle lineage (Housden et al., 2013; Krejci et al., 2009; Terriente-Felix et al., 2013). Based on cellular morphology and location of these Hnt-positive cells, I speculated that these cells may be related to the embryonic hemocyte lineage. Embryonic hemocytes originate in the head mesoderm and are often characterized as scattered, and having a round or irregular cellular morphology (Tepass et al., 1994). This description of embryonic hemocytes is similar to my observations of the scattered anterior Hnt-positive cells in the activated N embryos. Croquemort (Crq) is a macrophage receptor expressed in many embryonic hemocytes (Franc et al., 1996), and anti-Crq antibody is useful as a marker for this cell type. By performing anti-Crq, Hnt double immunostaining on the N activated embryos; the anterior scattered Hnt-positive cells were found to also be Crq-positive (Fig. 3.2A-C). This result is consistent with *hnt* being a N-responsive gene in the embryonic hemocyte lineage. This novel observation is consistent with previous findings suggesting that *hnt* functions as a N-responsive gene within the larval hemocyte lineage, the origin of which is distinct from the embryonic lineage. Overall, these results suggest the transcriptional activation of *hnt* by N signaling is highly tissue-specific.

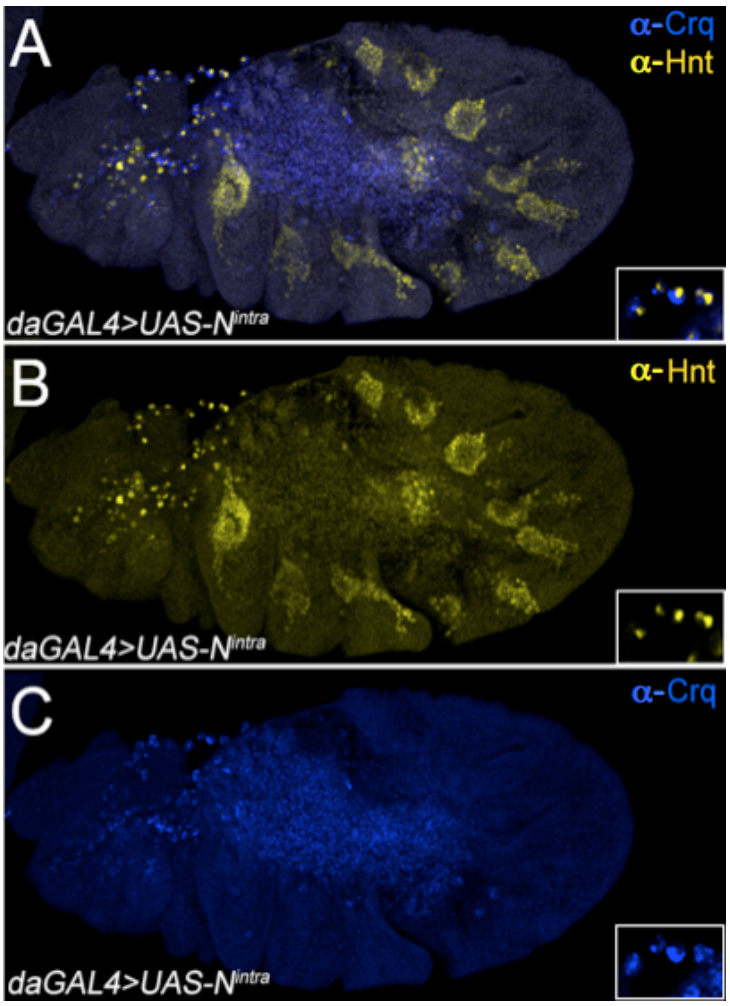

Figure 3.2 Hnt is responsive to activated N in embryonic hemocyte-like cells
Embryos overexpressing an activated form of N were double-immunostained using anti-Hnt, Crq. All of the anterior scattered Hnt-positive cells, marked by nuclear immunostaining of Hnt (B), show cytoplasmic anti-Crq immunostaining (A, C), indicating that these cells are related to the hemocyte/macrophage lineage. The inset located at the bottom right corner of each panel displays a zoomed-in section of the anterior Hnt-positive scattered cells.

3.2 Analysis of *hnt* mutant embryos

As described previously, Hnt is required for various morphogenetic processes in addition to cellular differentiation throughout development. To further characterize and identify functions that require Hnt, embryos of a *hnt* antibody-null allele used in many previous publications (Lamka and Lipshitz, 1999; Pickup et al., 2002; Reed et al., 2001; Wilk et al., 2000; Yip et al., 1997), hnt^{XE81}, were analyzed. In comparison to wildtype embryos (Fig. 3.3A), the neurons of hnt^{XE81} embryos, visualized by anti-22C10 immunostaining, displayed a reduction in the number of neurons associated with the lch5 chordotonal cluster (Fig. 3.3B). Three neurons were present along each lateral cluster of hnt^{XE81} embryos in contrast to five neurons normally found in wildtype embryos (Fig. 3.3C, D, white arrowheads). Intriguingly, this exact reduction of neurons from five to three has been previously described for mutants of the EGFR signaling pathway, including *rho*, *spi*, and *egfr* (Lage et al., 1997; Okabe and Okano, 1997; Rusten et al., 2001). The entire chordotonal structure in wildtype and hnt mutant embryos was also examined using a DPax2-GFP reporter. This revealed that two entire chordotonal organs, not just their associated neurons, were absent in *hnt* mutants (Fig. 3.3E-H, asterisks).

The recruitment of oenocytes, which as described in Chapter 1 is also an EGFR-dependent process, was also found to be severely impaired in hnt^{XE81} embryos. This analysis used the oenocyte-specific driver, *BO-GAL4*, in combination with $UAS\text{-}GFP^{nls}$ (Fig. 3.3J). In wildtype embryos, seven *BO-GAL4*-positive (from here on referred to as BO-positive) clusters were present, with each cluster containing a minimum of six cells (Fig. 3.3I). In *hnt* mutants, the overall number of BO-positive clusters was reduced and the clusters were frequently dispersed. In addition, the overall number of BO-positive

cells, which was expected to be a minimum of n=42 for each lateral side of the embryo, was reduced to n=26 (Fig. 3.4). Curiously, in *hnt* mutant embryos many of the BO-positive cells were improperly located in the anterior region of the embryo. These displaced BO-positive cells could represent non-specific BO-GAL4 expression, or they could reflect a defect in cell adhesion (see discussion). The impairment of oenocyte recruitment as well as the reduction of numbers in the lateral chordotonal organ clusters has not been previously reported and is consistent with the possibility that Hnt is required for these EGFR-dependent processes.

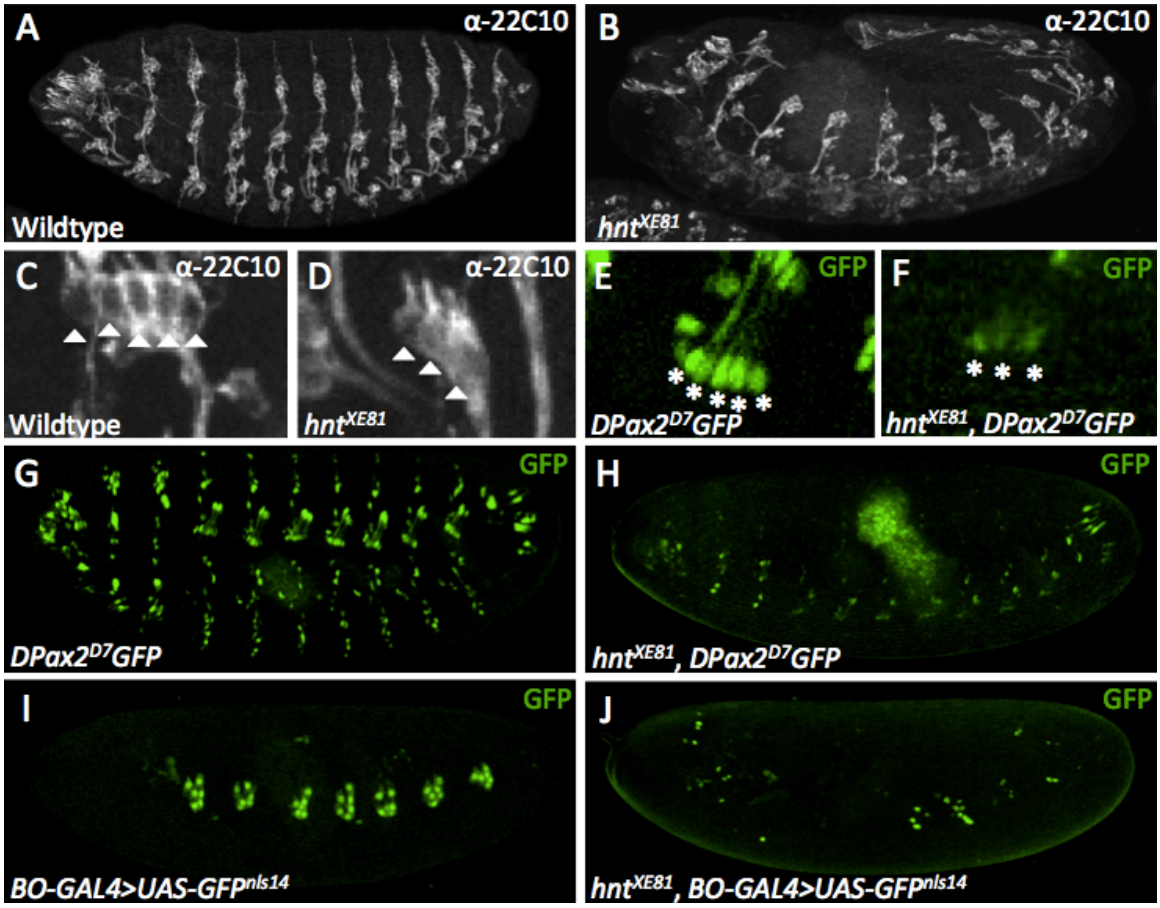

Figure 3.3 *hnt* mutant embryos display impairment during chordotonal organ and oenocyte recruitment

Analysis of neuronal phenotypes (A-D) and chordotonal phenotypes (E-H) in wildtype (A, C, E, G, I) and in hnt mutant embryos (B, D, F, H, J). The neuronal outlines in wildtype (A) and *hnt* mutant (B) embryos were visualized via anti-22C10 immunostaining. Wildtype chordotonal organs display a pentascolopodial structure, consisting of 5 neurons (C, white arrowheads). In *hnt* mutants, scolopodial neurons are reduced in number, from 5 to 3 neurons (D, white arrowheads). Chordotonal organs, visualized using DPaxD7GFP, are also reduced in number in *hnt* mutants (F, asterisks) compared to wildtype embryos (E, asterisks). Oenocytes, visualized using *BO-GAL4* expressing nuclear GFP, are similarly reduced in number in hnt mutants (J) compared to wildtype (I).

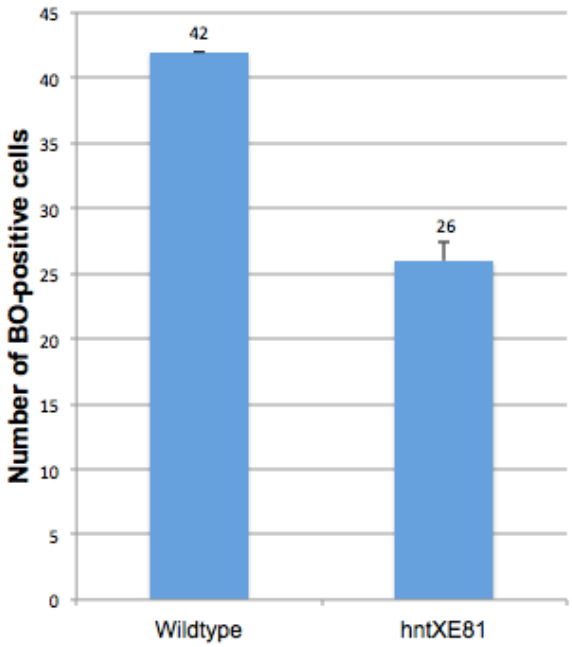

Figure 3.4 Reduction of oenocytes in *hnt* mutants
A comparison of the number of BO-GAL4 expressing nuclear GFP (BO-positive) cells, representing oenocytes, in wildtype and *hnt* mutant (hnt^{XE81}) embryos. In wildtype embryos (3 embryos examined), 42 BO-positive cells were consistently present as seven clusters of six cells per lateral side. In *hnt* mutant embryos (2 embryos examined), approximately 26 BO-positive cells were present, including those that were dispersed throughout the embryo.

3.3 Requirement of EGFR signaling for embryonic HNT expression

The previous section (see Section 3.2) described some striking similarities in the phenotypes of *egfr* and *hnt* mutant embryos. One possibility that would be consistent with these observations would be a requirement of EGFR signaling for Hnt expression. Thus, to determine whether embryonic Hnt expression was dependent on EGFR signaling, Hnt expression was analyzed in *egfr* mutants using anti-Hnt immunostaining (Fig. 3.5A). In the absence of *egfr*, Hnt expression appeared to be EGFR-independent in several tissues. This, however, does not rule out the possibility that some embryonic Hnt expression could be EGFR-dependent. To examine this possibility, an activated EGFR ligand, secreted Spitz (sSpi), was expressed throughout the embryo using the *daGAL4* driver. These embryos were immunostained for Hnt, revealing massive ectopic Hnt expression throughout the dorso-lateral region of the embryo (Fig. 3.5B). It has been previously shown that overexpression of secreted Spitz (sSpi) can induce supernumerary oenocyte recruitment (Elstob et al., 2001). Given that Hnt is strongly expressed in oenocytes, the observed ectopic expression could represent these supernumerary oenocytes. Therefore, the effect of overexpressing sSpi on the induction of Hnt expression could be indirect. Interestingly, a very similar effect was seen using a downstream component of the EGFR signaling pathway, *UAS-RasD*^{V12}, which is an activated form of Ras. Overexpression of activated Ras with *daGAL4* also resulted an expansion of Hnt expression in the dorso-lateral region of the embryo (Fig. 3.5C). Overall, these results suggest that EGFR signaling may promote, but may not be required for Hnt expression during *Drosophila* embryogenesis.

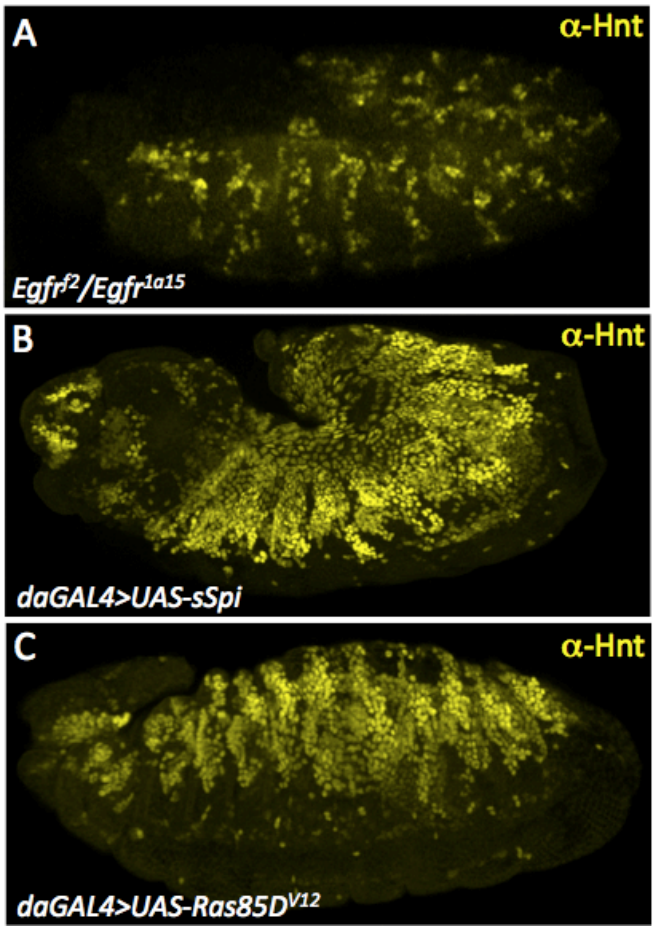

Figure 3.5 EGFR signaling is not required for, but can promote, Hnt expression
Hnt expression persists in *egfr* mutant embryos (A), suggesting that EGFR signaling is not an absolute requirement for embryonic Hnt expression. However, ubiquitous overexpression of secreted Spitz (sSpi) induces ectopic Hnt expression in the lateral region of the embryo (B). Similarly, overexpression of activated Ras ($Ras85D^{V12}$) also induces ectopic Hnt expression (C), suggesting that EGFR signaling can promote Hnt expression in this region of the embryo.

3.4 Ectopic DPax2 induction in Hnt overexpressing embryos

Several studies have described hnt mutant phenotypes in various tissues. Yet, Hnt's role as a potential transcription factor and its transcriptional targets remain poorly characterized. Previous work in our lab involving a microarray analysis of embryos overexpressing Hnt identified numerous putative transcriptional targets. Among the many candidate genes identified, *DPax2* was one of most interest. Upon strong overexpression of Hnt, it was found that DPax2 could be induced throughout the embryo (Fig. 3.6D-D") (Du, 2013). Interestingly, Hnt and DPax2 are both strongly expressed during the development of the PNS during embryogenesis, and both genes have been identified as genes being significantly upregulated in the SOP lineage (Bufflin and Gho, 2010; Reeves and Posakony, 2005). Further to these studies and observations, I investigated the possibility that DPax2 is a direct target of Hnt, in addition to investingating signaling pathways that could mediate the effect of Hnt overexpression on DPax2 expression.

3.4.1 The *sv* promoter is responsible for the induction of DPax2 upregulation during Hnt overexpression

In hopes of finding an accurate DPax2 reporter to visualize embryonic DPax2 expression faithfully as seen with DPax2 immunostaining (Fig. 3.6A), embryonic expression patterns of several GFP or RFP-tagged DPax2 reporter lines (provided by Dr. Joshua Kavaler, Colby College, Maine) were characterized (see Appendix B). These reporters carry various regions of the large *shaven* (*sv*) enhancer, spanning approximately 6.7 kb upstream of *DPax2* (Johnson et al., 2011). These reporters allow DPax2 expression to be analyzed via live-imaging of embryos and other tissues, and provides a cost and time-efficient method of visualizing gene transcription. In total, seven reporter lines were examined. Among the seven, the B reporter line, $DPax2^{B1}$, was found to be most faithful to endogenous DPax2 expression during embryonic development (Fig. 3.6A-C). The $DPax2^{B}$ reporter constructs are comprised of a 3.1 kb portion of *sv*, as well as 100 bp of the 5' UTR of *DPax2* (Johnson et al., 2011). To determine whether this reporter construct is also overexpressed in embryos overexpressing Hnt, its expression was examined in the *daGAL4>UAS-GFP-*$HNT_{(II)}$ background (Fig. 3.6E-E"). Interestingly, the same phenotype of ectopic DPax2 induction was observed, indicating that the regulatory region that is responsive to Hnt overexpression is contained within this 3.1 kb region as described above.

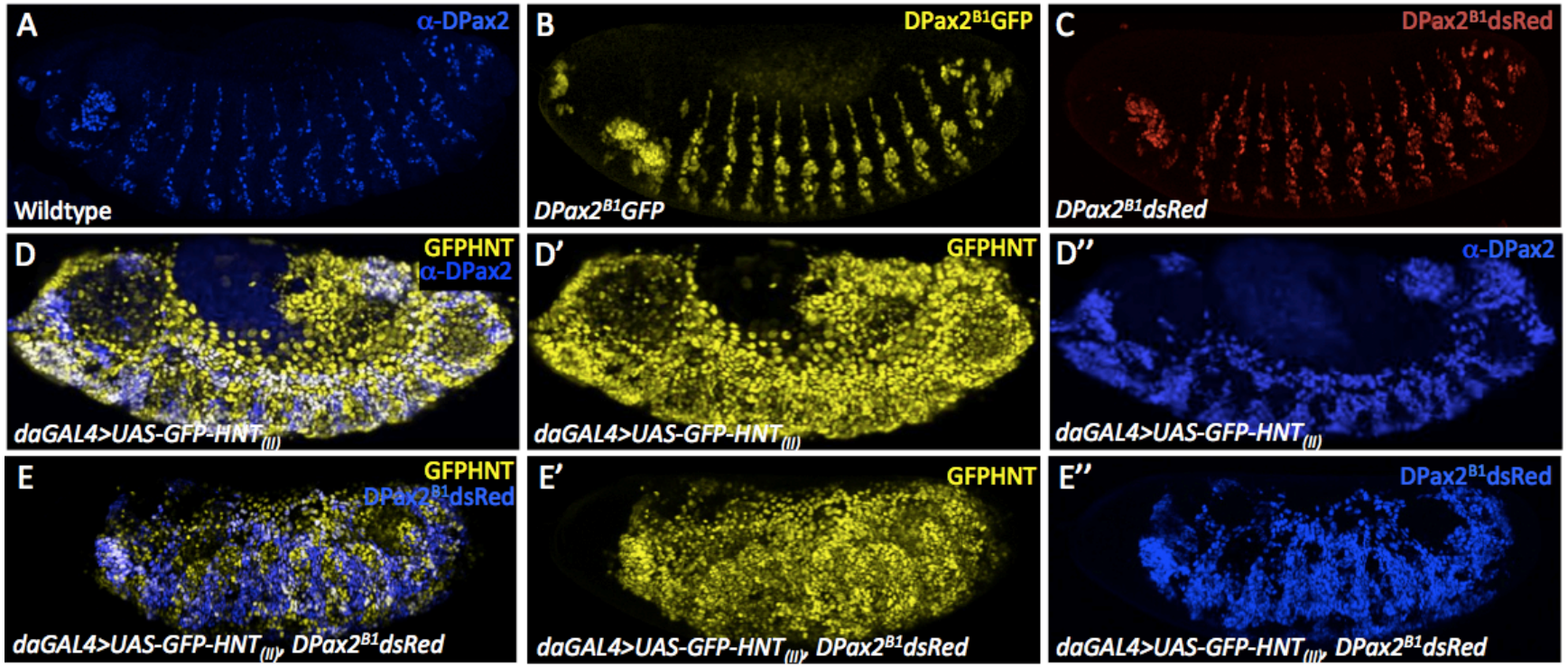

Figure 3.6 DPax2 is responsive to Hnt overexpression through the *sv* enhancer
Wildtype embryonic DPax2 expression (A-C), visualized via anti-DPax2 immunostaining (A, blue) and DPax2^{B} reporter lines, DPax2^{B1}GFP (B, yellow), and DPax2^{B1}dsRed (C, red). Embryos ubiquitously overexpressing GFP-HNT$_{(II)}$ showing DPax2 overexpression by anti-DPax2 immunostaining (D-D"; provided by Y. Du (Du, 2013)). Embryos ubiquitously overexpression GFP-HNT$_{(II)}$ showing DPax2 overexpression detected using the DPax2^{B1}dsRed reporter (E-E").

3.4.2 Induction of ectopic DPax2 is highly dependent on levels of Hnt

Previous studies in our lab have shown an apparent threshold effect with respect to the induction of DPax2 expression by Hnt overexpression. In particular, ectopic DPax2 expression was found to only be induced in the context of high levels of Hnt overexpression (Du, 2013). To investigate this effect further, similar experiments were performed utilizing three GAL4-responsive *hnt* lines that are associated with lower levels of Hnt overexpression when compared to the *UAS-GFP-HNT$_{(II)}$* line. Among the three lines, two UAS-responsive P-element insertions (so called enhancer-promoter lines), *EP55* and *GS1018*, were used. In addition, an independent insertion of the same UAS-GFP-HNT construct mapping to the third chromosome, *UAS-GFP-HNT$_{(III)}$*, was used. Previous results from our lab have shown that *EP55* crossed to *daGAL4* is unable to induce DPax2 expression (Du, 2013). If a threshold effect is in place, increased expression of EP55 should be able to induce DPax2 expression. To test this hypothesis, two GAL4 drivers, *Act5cGAL4* and *daGAL4*, were used simultaneously to drive expression of *EP55*. Strikingly, expression of EP55 using the two GAL4 drivers did not induce DPax2 expression throughout the lateral epidermis, but did result in ectopic DPax2 expression in the embryonic salivary gland (Fig. 3.7A). In wildtype embryos, DPax2 expression as evaluated by immunostaining or DPax2 reporter expression is never observed in the embryonic salivary gland (see Fig. 3.6A-C). Ectopic salivary gland expression of DPax2 was also observed when *GS1018* or *UAS-GFP-HNT$_{(III)}$* was overexpressed with *daGAL4* (Fig. 3.7B,C). Other studies in our lab of Hnt overexpression have indicated that these different UAS-responder lines are associated with different levels of Hnt expression, where *UAS-GFP-HNT$_{(II)}$* is the strongest, *GS1018*

and *UAS-GFP-HNT$_{(III)}$* are intermediate, and *EP55* is the weakest (data not shown, B.H.R. personal communication). Overall, these results demonstrate that the level of Hnt required to induce DPax2 expression varies depending on tissue-specificity. Interestingly though, the embryonic salivary gland displays the lowest threshold for HNT-dependent ectopic DPax2 expression.

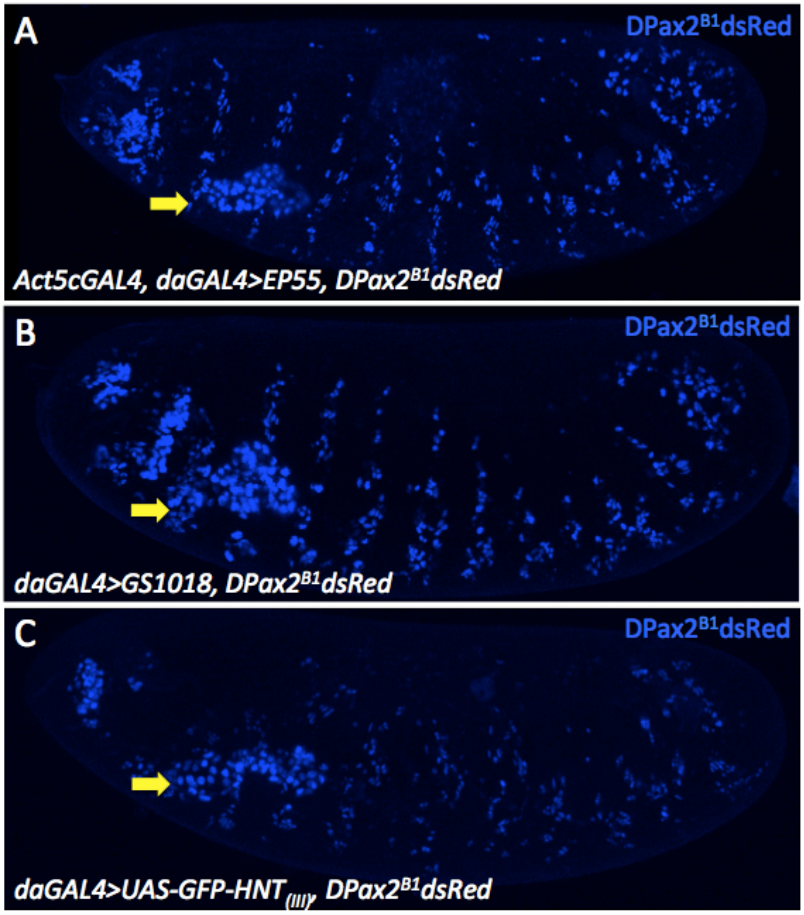

Figure 3.7 Ectopic DPax2 expression is sensitive to levels of Hnt overexpression
Embryos showing DPax2 expression, via the DPax2^{B1}dsRed reporter, using three different GAL4-responsive Hnt constructs, each of which is weaker than *UAS-GFP-HNT$_{(II)}$* (see text). Overexpression of EP55 using 2 GAL4 drivers to elevate expression induces ectopic DPax2 in the embryonic salivary gland, as marked by the yellow arrow (A). Similarly in embryos overexpressing GS1018 (B) and GFP-HNT$_{(III)}$ (C), DPax2 expression is induced in the salivary gland, as marked by the yellow arrow (compare to Fig. 3.6A-C).

3.5 Examining the mechanism of ectopic DPax2 expression in HNT overexpressing embryos

The suggested functional conservation between Hnt and its mammalian homolog, RREB1, allows speculatation that Hnt can function as either a transcriptional potentiator or attenuator to regulate the expression of its target genes (Ming et al., 2014). Our studies on DPax2 expression suggest that this gene could be directly activated by high levels of Hnt. However, it is also possible that Hnt's effect on DPax2 expression is indirect. Interestingly, in pupal eye development, Hnt has been reported to be required non-autonomously for cone cell (CC) induction, which is dependent on DPax2. This model for CC induction has been described in Chapter 1, and indicates that DPax2 expression, through the *spa* enhancer, requires three key inputs from N, EGFR, and Lz (Fig. 3.8A) (Flores et al., 2000). Since the overexpression of Hnt interacts with the *sv* enhancer, and the regulation of DPax2 activation through *sv* is not well-defined, inputs from the model for CC induction were tested. Two of three inputs are highly conserved signaling pathways during metazoan development, and thus, DPax2 expression in embryos overexpressing Hnt was tested in the absence of the i) N signaling pathway (Fig. 3.8B) or ii) EGFR signaling pathway (Fig. 3.8C).

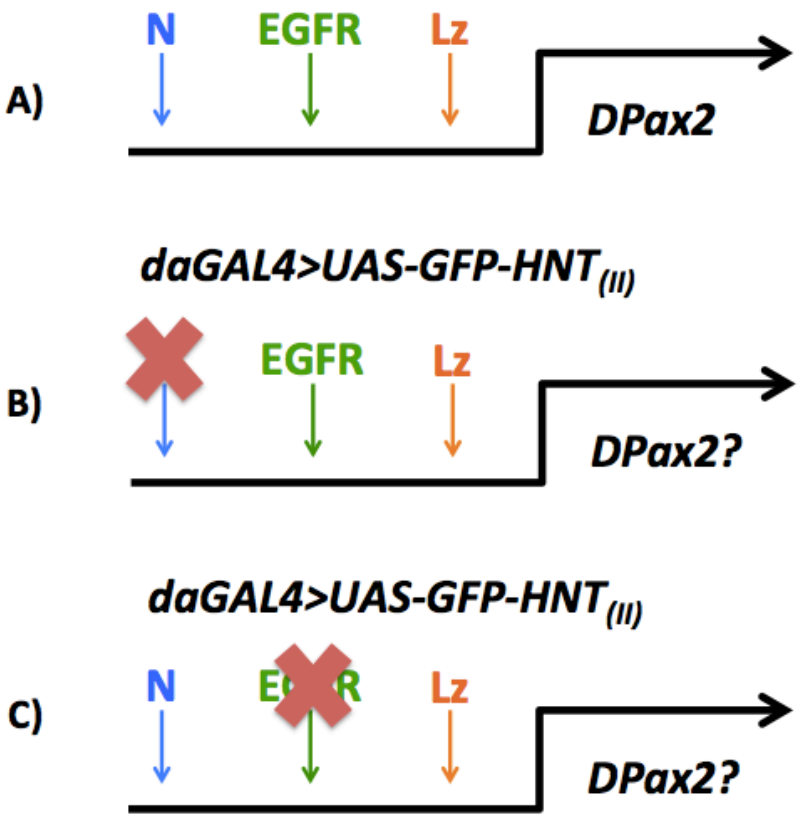

Figure 3.8 The model for DPax2 expression during CC induction
(A) The model for CC induction as described by Flores et al. (2000). Activation of DPax2 expression requires inputs from N and EGFR signaling, and Lz. To test whether Hnt is dependent on either N or EGFR to activate ectopic DPax2 expression, Hnt overexpression will be tested in *N* mutant (B) or *egfr* mutant (C) backgrounds

3.5.2 EGFR signaling is required to induce ectopic DPax2 expression in Hnt overexpression embryos

To test if DPax2 expression is activated indirectly as a consequence of Hnt overexpression, *UAS-GFP-HNT$_{(II)}$* was overexpressed with *daGAL4* in *N* and *egfr* mutant embryos. In *N^{55e11}* mutant backgrounds, the absence of N signaling did not affect Hnt's ability to induce ectopic DPax2 expression (Fig. 3.9A-A"), suggesting that N signaling does not mediate this response. However, in this context, the induced DPax2 expression was localized only in the lateral region of the embryo, despite Hnt being overexpressed throughout the embryo. This clustering effect may relate to the neurogenic phenotype of *N^{55e11}* mutants (recall Fig. 3.1C), and is suggestive that ectopic DPax2 induction through Hnt overexpression is restricted to the PNS lineage.

Since DPax2 induction in the context of Hnt overexpression is not dependent on N signaling, the Hnt overexpression effect on DPax2 expression was subsequently analyzed in *egfr* mutant embryos. Strikingly, ectopic DPax2 expression, as visualized using the DPax2^{B1}dsRed reporter, was completely suppressed in *egfr* mutant embryos overexpressing Hnt (Fig 3.9B-B"). In these embryos, which were highly abnormal in their development, some endogenous DPax2 expression was observed - presumably in the degenerating PNS. DPax2 expression in *egfr* mutant embryos lacking Hnt overexpression was also examined using the DPax2^{B1}dsRed reporter (Fig. 3.9C), and was found to be similar to *egfr* mutant embryos overexpressing Hnt, although in the absence of Hnt overexpression, PNS development was not as irregular.

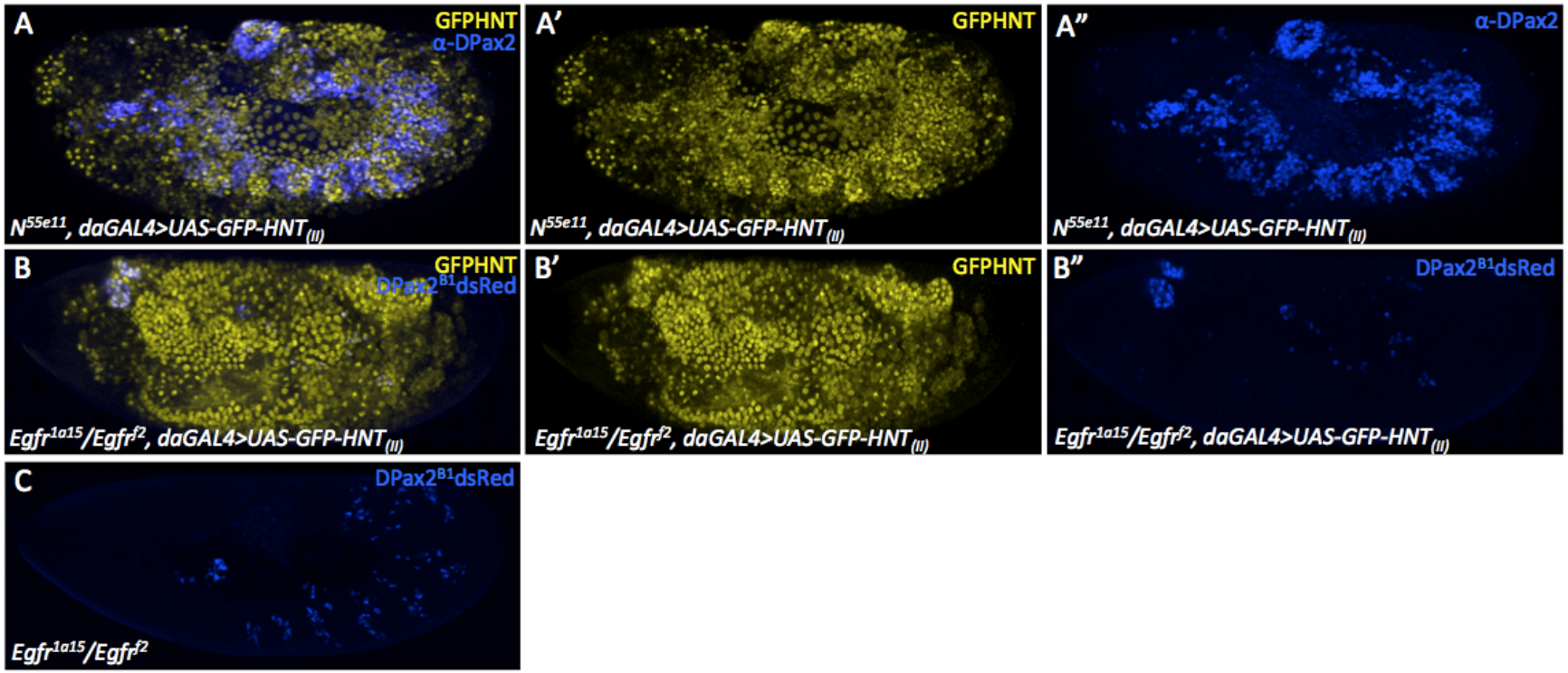

Figure 3.9 Induction of ectopic DPax2 expression through Hnt overexpression is dependent on EGFR signaling and does not require N signaling

Hnt overexpression was visualized by GFP-HNT$_{(II)}$ (A, A', B', B', yellow) and DPax2 expression was visualized by anti-DPax2 immunostaining (A", red) or DPax2^{B1}dsRed reporter expression (B", C, red). Embryos overexpressing GFP-HNT$_{(II)}$ in *N* mutant embryos display strong DPax2 expression (A"). Strikingly, *egfr* mutants overexpressing GFP-HNT$_{(II)}$ does not show ectopic DPax2 expression (B"). In *egfr* control mutant embryos, DPax2 expression is reduced but is detectable (C).

3.5.3 Levels of Hnt and EGFR combinatorially control ectopic DPax2 induction

As discussed in Section 3.4.2, ectopic DPax2 expression is only induced upon high levels of Hnt overexpression. To determine if this effect is dependent on levels of EGFR signaling, induction of ectopic DPax2 expression was assessed in embryos heterozygous for the *egfr* mutant allele, $egfr^{f2}$, as well as embryos overexpressing dominant-negative Ras. In heterozygous *egfr* mutants overexpressing Hnt, DPax2 induction was visibly reduced (Fig. 3.10A-A"). A similar result was found in embryos simultaneously overexpressing $UAS\text{-}GFP\text{-}HNT_{(II)}$ and a dominant negative form of Ras, $UAS\text{-}Ras85D^{N17}$ (Fig. 3.10B-B"). These results support the idea that the requirement of a high level of Hnt expression for the induction of DPax2 is further dependent on the level of EGFR signaling, as the induction effect can be partially suppressed by reducing EGFR gene dosage or dominantly suppressing downstream effectors of Ras.

The above results suggest that levels of EGFR signaling are able to impact DPax2 expression. Subsequently, it was of interest to test whether activation of the EGFR signaling pathway can induce DPax2 overexpression without Hnt overexpression. Using the DPax2B1GFP reporter, embryos driving the expression of $Ras85D^{V12}$ (activated Ras) with *daGAL4* were found to be associated with some expansion of DPax2 expression (Fig. 3.10C). Similar activation of the EGFR signaling pathway can be achieved by expressing the activated ligand, sSpi, and such embryos were also found to show expanded DPax2 expression (Fig. 3.10D). Given that embryos overexpressing a low level of Hnt do not result in inappropriate DPax2 expression (associated with the *EP55* insertion as described in Section), it was of interest to determine if EP55 could enhance the effect of activated Ras. Again, using the $DPax2^{B1}GFP$ reporter, co-expression of

EP55 and Ras85D^{V12} resulted in increased DPax2 expression beyond what was observed when expressing Ras85D^{V12} on its own (Fig. 3.10E). This observation is consistent with Hnt's function being to potentiate or enhance the activity of the EGFR signaling pathway.

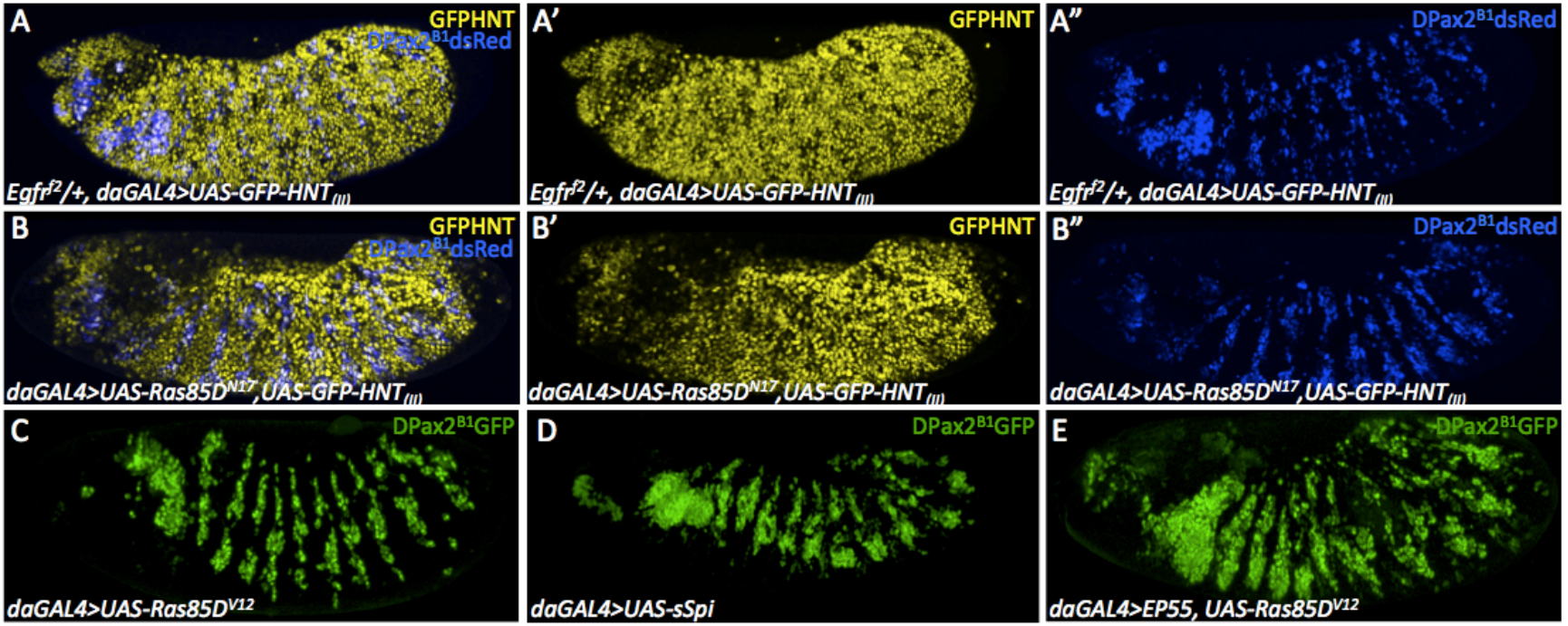

Figure 3.10 EGFR signaling and Hnt work cooperatively to induce DPax2 expression in the embryo
Embryos heterozygous for a *egfr* mutant allele, $Egfr^{f2}$, overexpressing GFP-$HNT_{(II)}$ show a significant reduction of ectopic DPax2 expression (A-A"). A similar reduction in ectopic DPax2 expression is observed in embryos simultaneously expressing a dominant negative form of Ras, Ras85DN17, and GFP-$HNT_{(II)}$ (B-B"). Embryos overexpressing components of EGFR signaling, either activated Ras, $Ras85D^{V12}$ (C) or secreted Spitz (D), show expanded DPax2 expression without Hnt overexpression. However, co-expression of $Ras85D^{V12}$ and EP55 results in a higher degree of expansion of DPax2 expression (E).

3.6 Examining the responsiveness of DPax2 to Hnt in the pupal retina

Both Hnt and DPax2 are endogenously expressed in multiple cell types during retinal development. Wildtype Hnt expression is present in all neuronal precursor cells in third instar eye discs (Pickup et al., 2002). In a 48 hr after puparium formation (APF) pupal retina, Hnt expression is present in the R cells (R1-R8) and the neuronal cell within the interommatidial SOP lineage. Wildtype DPax2 expression is confined to the CCs, 1°s, and the interommatidial bristles. To assess whether Hnt can ectopically induce DPax2 expression in a different tissue context, the developing retina was chosen. Embryonic expression of Hnt and DPax2 show complementary expression patterns in the developing embryonic PNS during the differentiation of the SOP lineage (Fig. 3.11A-A"). Similarly in the retina, within the interommatidial SOP cells, Hnt and DPax2 display complementary expression patterns (Fig. 3.11B-B"). Additionally, as mentioned in Chapter 1, it has been stated that the specification of the chordotonal SOPs is analogous to the development of the interommatidial SOPs (Lage et al., 1997). Therefore, one possible mode of action for the cause of DPax2 induction upon Hnt overexpression is that the SOP cells are highly sensitive to Hnt or EGFR levels, leading to an activation of DPax2 expression.

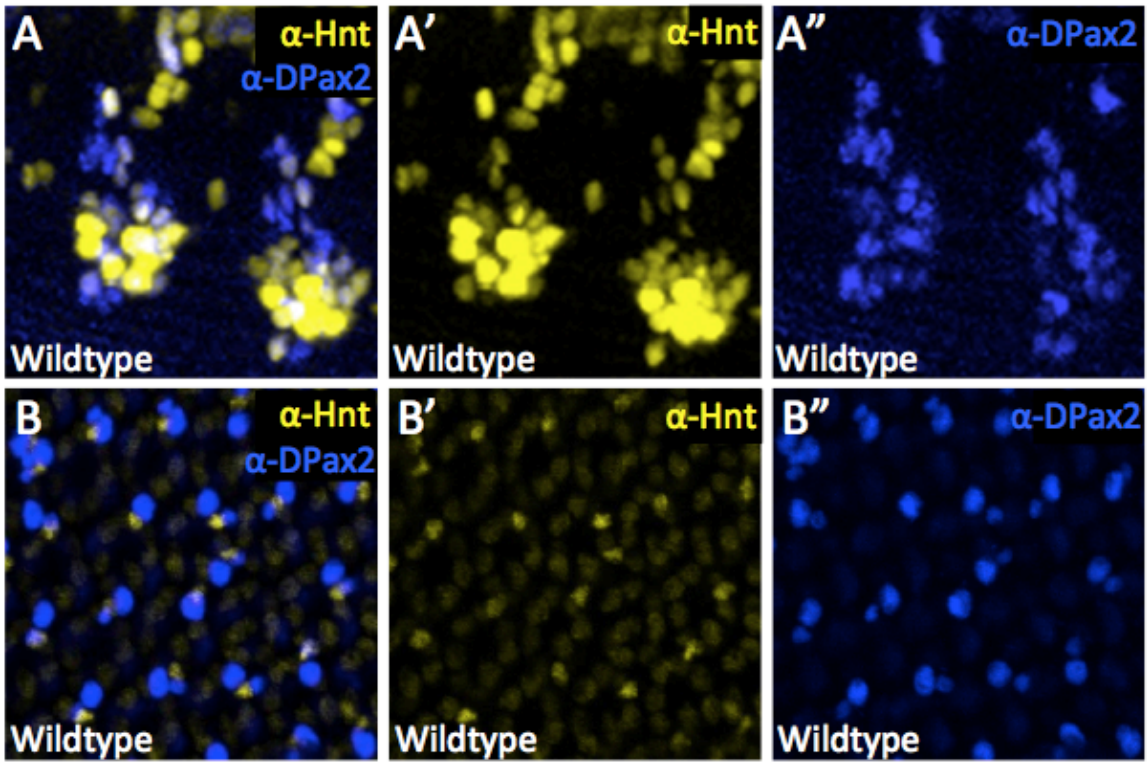

Figure 3.11 Hnt and DPax2 expression is infrequently co-expressed and often close proximity in the developing PNS of wildtype retinas and embryos
Embryos (A) and retinas (B) immunostained with anti-Hnt (A, A', B, B', yellow) and anti-DPax2 (A, A", B, B", blue) showing endogenous PNS expression patterns of Hnt and DPax2. All pupal retinas were staged at 48 hours after puparium formation (APF). Co-immunolocalization (indicated by white in panels A and B) is not prominent.

3.6.1 Overexpression of Hnt induces DPax2 expression in the pupal retina through the *sv* promoter

Since embryonic DPax2 expression is responsive to the overexpression of Hnt through the *sv* promoter, it was of interest to determine whether the same mechanism is utilized in the pupal eye. As mentioned in Section 3.4.1, DPax2^{B} reporters contain a fragment of the *sv* promoter, which has been characterized in the development of bristles (Johnson et al., 2011). Interestingly, upon comparison of wildtype DPax2 immunostaining (Fig 3.12A-A") and DPax2^{B1}dsRed expression in the eye, DPax2^{B1}dsRed expression was detected in the interommatidial SOP cells and CCs (Fig. 3.12B-B",C-C"). However, unlike the expression of endogenous DPax2, which is expressed in all four CCs (Fig. 3.12A'), the expression of the DPax2B1dsRed reporter was most frequently observed in only one CC (Fig. 3.12B-B").

To assess whether DPax2 is responsive to overexpression of Hnt in the pupal retina, the *GMR-GAL4* driver was utilized. The *Glass-Mediated-Response* (*GMR*) synthetic promoter element specifically promotes expression throughout eye morphogenesis in most cell types (Brand and Perrimon, 1993). Overexpression of Hnt using *GMR-GAL4* resulted in larval lethality (data not shown) and, therefore, the GAL80^{ts} system (see Chapter 2) was utilized to induce overexpression of Hnt 24 hr APF. Strikingly, this overexpression of Hnt induced ectopic DPax2 expression in the eye, detected by anti-DPax2 immunostaining (Fig. 3.13A-A"). Consistent with observations of DPax2^{B1}dsRed reporter expression in the embryo, DPax2^{B1}dsRed reporter was also responsive to Hnt overexpression throughout the retina (Fig. 3.13B-B"). However, DPax2 expression, as detected by immunostaining, was qualitatively different from the DPax2

reporter expression, where the latter shows areas devoid of expression (Fig. 3.13A",B" arrowheads). These areas presumably correspond to the CCs, which as stated previously, activate DPax2 reporter expression in only one of the four CCs. To visualize the arrangement of cells within the retinal epithelium, anti-Armadillo (Arm) staining was performed. This revealed that overexpression of Hnt under these conditions ($GAL80^{ts}$ shift 24 hr APF, from here on referred to as strong/late Hnt overexpression) did not disturb the specification of the CCs, but greatly disturbed the surrounding cells and the development of the interstitial lattice. Interestingly, based on morphology, most interstitial cells resembled primary pigment cells. The ectopic DPax2 expression resulting from Hnt overexpression could represent increased DPax2 expression in the primary pigment cells or ectopic expression in the lattice cells.

In a previous publication by Pickup et al. (2009), it has been stated that overexpression or reduction of Hnt in the larval eye discs can affect the expression of the transcription factor Cut, which is a marker for CCs. To determine if this was the case in the pupal eye, anti-Cut immunostaining was performed on the strong/late Hnt overexpression pupal retinas. This revealed an unusual localization of Cut in comparison to wildtype (Fig. 3.13D",E). Wildtype retinas display strong anti-Cut immunostaining in CC nuclei (Fig. 3.13E'), as well as the nuclei of the cells of the interommatidial SOP lineage (Fig. 3.13E"). In the Hnt overexpression retinas, Cut showed normal nuclear localization in CCs (Fig. 3.13D" arrow); immunostaining of Cut in the SOP lineage, however, showed very strong nuclear localization, in addition to localization throughout the developing interommatidial bristle cells. The failure of complete Cut nuclear localization is consistent with strong Cut overexpression, resulting in cytoplasmic

accumulation of this transcription factor. This result suggests that Hnt overexpression can result in increased Cut expression in the interommatidial SOP lineage. CC expression of Cut, however, was unaffected. This is most likely due to the timing of Hnt overexpression, which was induced 24 hr APF. At this developmental stage, CC specification has been completed (see Fig. 1.4) and these cells may no longer be competent to respond to Hnt overexpression.

.

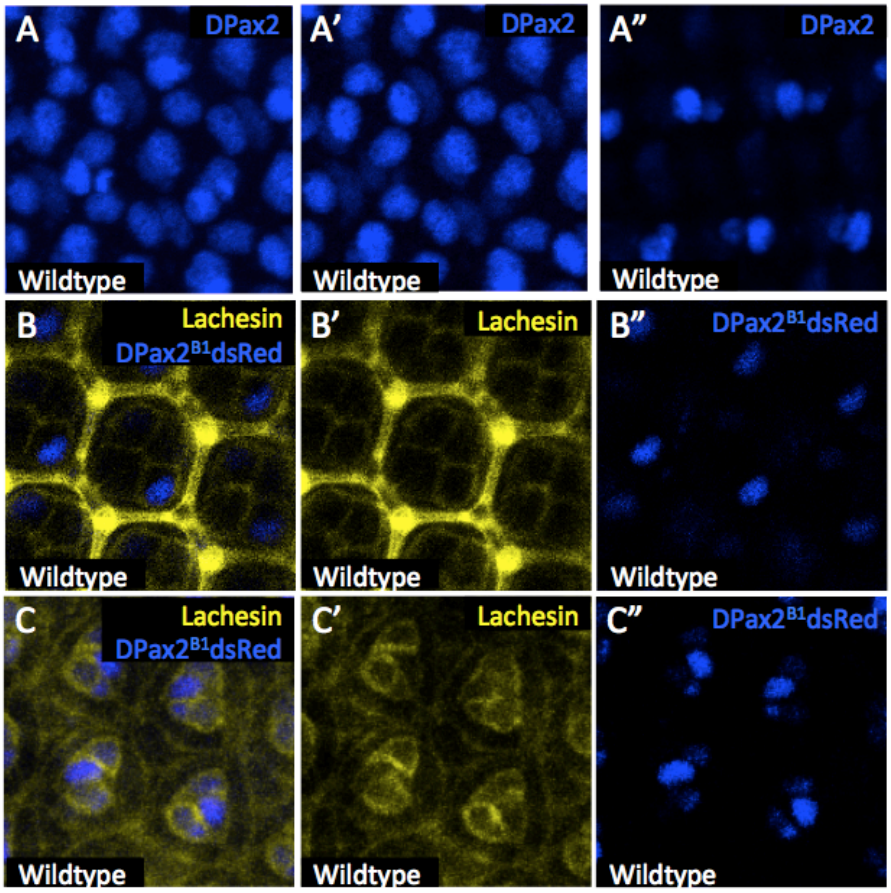

Figure 3.12 A comparison between DPax2 immunostaining and DPax2^{B1}dsRed reporter expression in the pupal retina

Wildtype anti-DPax2 immunostaining of pupal retinas 48 hr APF (A) displays strong DPax2 expression in all four CCs and weak expression in 1°s as seen in an apical focal plane (A'). DPax2 expression is also observed within the cells of the developing interommatidial SOPs as seen in a basal focal plane (A"). DPax2^{B1}dsRed reporter expression in pupal retinas 48 hr APF carrying a Lachesin-GFP reporter expression to visualize cell outlines (B, C) shows reporter expression is limited to one or two CCs as seen in an apical focal plane (B-B"). However, in the developing interommatidial SOP cells, DPax2^{B1}dsRed reporter reports strong expression of DPax2, remaining faithful to the endogenous expression of DPax2 as seen in a basal focal plane (C-C").

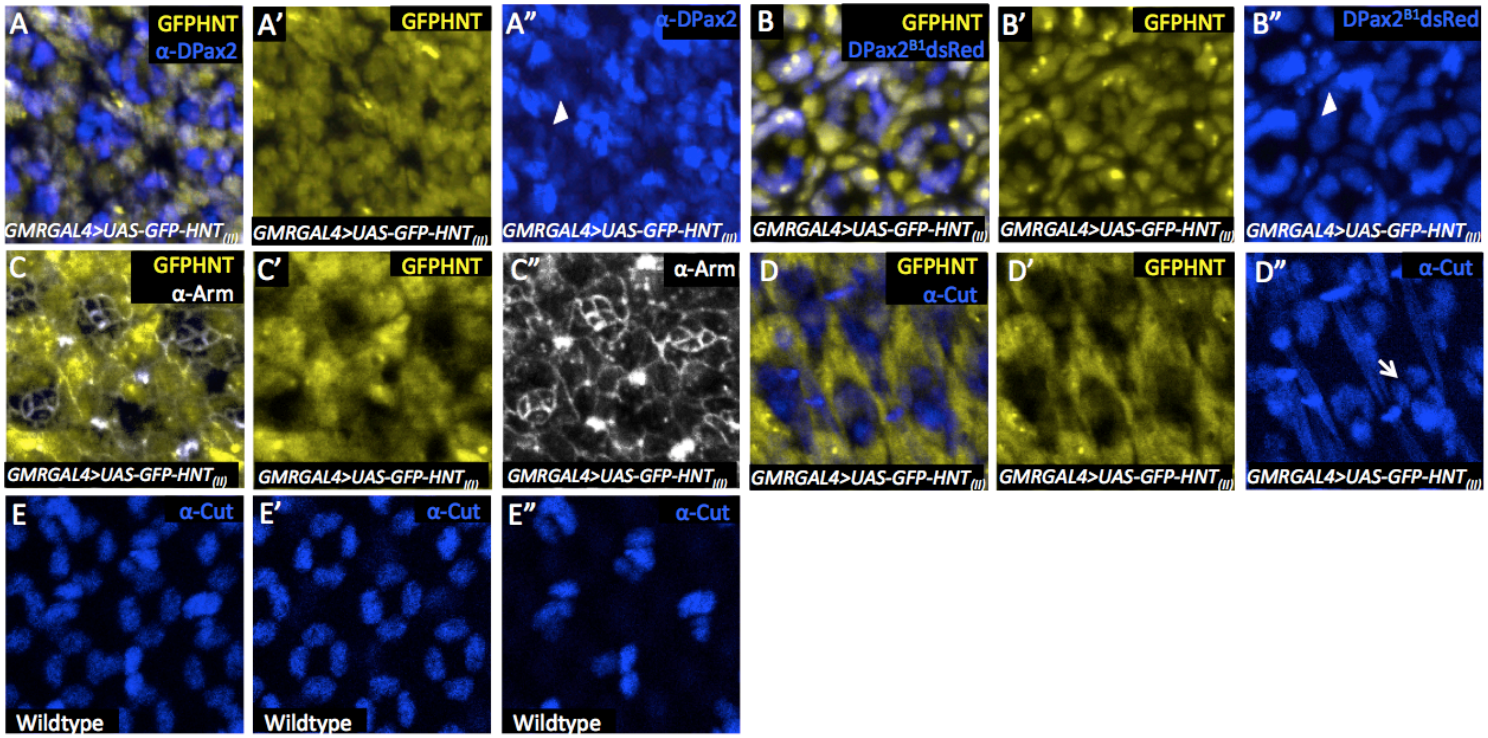

Figure 3.13 DPax2 is responsive to Hnt overexpression in the pupal retina through the *sv* promoter
Strong overexpression of Hnt induced 24 hours APF (A-D, see text) leads to induction of ectopic DPax2 expression, shown by anti-DPax2 immunostaining (A, A", blue) and DPax2^{B1}dsRed reporter expression (B, B", blue). Qualitative differences between the immunostaining (A") and reporter (B") are indicated by the white arrowheads (see text). Anti-Armadillo (Arm) immunostaining of the same background (C-C") showing cell outlines and revealing clusters of 4 CCs. Anti-Cut immunostaining in the overexpression background (D-D"), compared to wildtype (E-E"), shows inappropriate cytoplasmic localization of Cut throughout the developing bristle shaft and expression within CCs (D", arrow). Wildtype Cut is detected within all 4 CCs (E', apical) and the interommatidial SOP lineage (E", basal).

3.6.2 Temporal sensitivity of DPax2 to Hnt overexpression in the developing retina

The anti-Arm result in Section 3.6.1 was surprising in that CC specification did not appear to be disrupted. This may have been due to CC specification being an early event during differentiation of the pupal retina, and induction of Hnt 24 hr APF is likely too late to disrupt this process. To address whether Hnt overexpression is capable of disrupting CC specification, a weaker *UAS-GFP-HNT* insertion (*UAS-GFP-HNT*^{J27}), which is viable with *GMR-GAL4*, was used. Since this is a viable GAL4-UAS combination, a lower level of Hnt overexpression occurs earlier in the development of the pupal retina and the consequences on the development of the retinal epithelium can be evaluated 48 hr APF. To confirm if the viable *GMR-GAL4>UAS-GFP-HNT*^{J27} pupae are associated with ectopic DPax2 expression, the DPax2^{B1}dsRed reporter was crossed with this background. As expected, this resulted in upregulation of DPax2 expression, although this was qualitatively different from the induction of strong/late Hnt overexpression. In particular, the degree of ectopic DPax2 expression was less, but larger strongly expressing cells were observed (Fig. 3.14A-A"). While the GAL80^{ts} shift experiment did not disrupt CC specification, the early/weak Hnt overexpression may have resulted in increased DPax2 expression in CCs, either through enhanced expression in specified CCs or through the production of supernumerary CCs. To address this question, the early/weak Hnt overexpression background (*GMR-GAL4>UAS-GFP-HNT*^{J27}) was crossed to *Ubi-DE-Cadherin-GFP* to visualize apical membranes (Fig. 3.14C). The organization of the retinal epithelium was very different from the above GAL80^{ts} shift experiment (see Fig. 3.13C) as well as the wildtype epithelium (Fig. 3.14B), in that the typical CC cluster arrangement was not observed. Based on this

morphology, it is likely that the early/weak Hnt overexpression result is associated with supernumerary CCs, and this was confirmed using a CC-specific marker, anti-Cut (Fig. 3.14D).

.

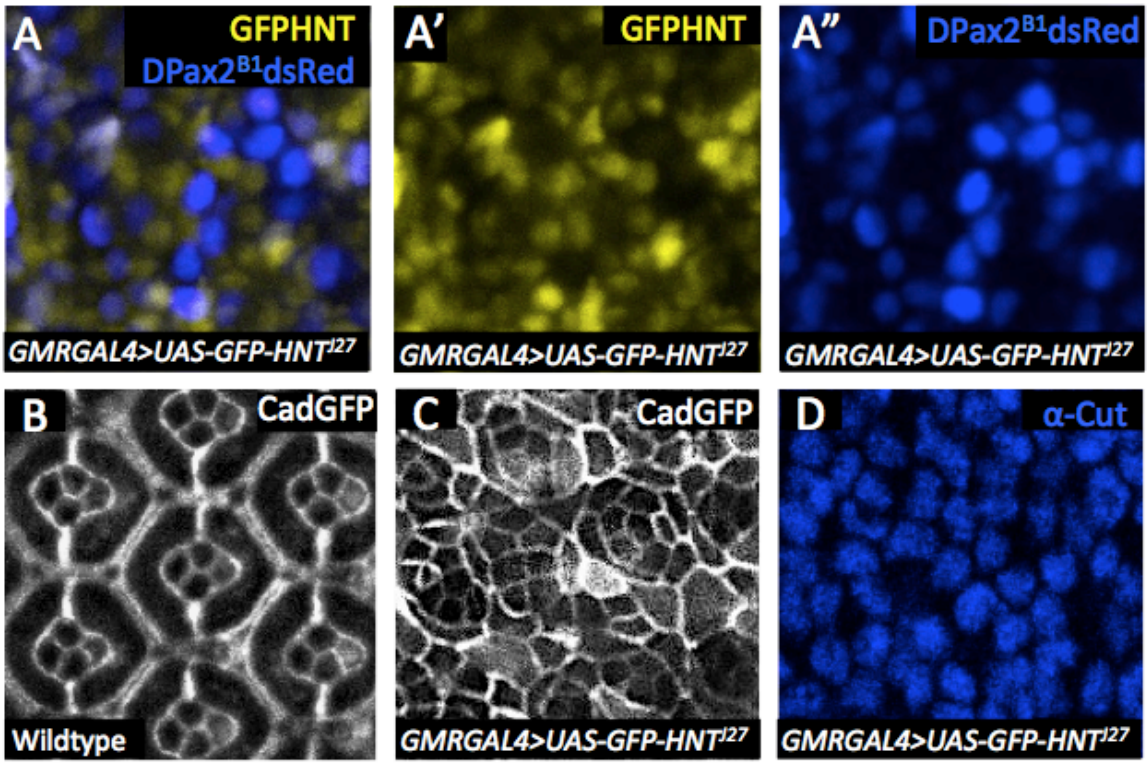

Figure 3.14 Early, weak overexpression of Hnt induces supernumerary CC differentiation
Pupal retinas associated with weak Hnt overexpression imaged 48 hr APF (*GMR-GAL4>GFP-HNT*^{J27}, see text) (A, C, D) show disruptions in the retinal epithelium compared to wildtype (B). Strong DPax2^{B1}dsRed reporter expression is seen (A", compare to Fig. 3.12B") in addition to a strong disruption of the cellular organization, visualized using Cadherin-GFP (C). Compared to the apical focal plane of wildtype (B), the cell outlines as displayed by Cadherin-GFP in the Hnt overexpressing pupal retina suggest supernumerary CC formation, confirmed by anti-Cut immunostaining (D).

3.7 Analysis of the pupal retina in *hnt*^{peb} mutants

In the developing retina, Hnt plays a critical role in the maintenance of epithelial integrity, establishment of planar polarity, and proper formation of photoreceptor cell morphology (Pickup et al., 2002). In previous publications, the phenotype of the pupal retinal epithelium of *hnt* mutants was not examined in detail. Therefore, pupal eyes of a viable temperature-sensitive *hnt* mutant, *hnt*^{peb}, were immunostained with anti-Arm to outline the apical cell membranes. In a 48 hr APF wildtype retinas, each ommatidium consist four CCs, two 1°s, six 3°s, three 3°s, and three bristle cells (Fig. 3.15A,A'), which are on the apical surface of the ommatidium, and located basally to the apical surface are eight R cells. In comparison to the wildtype ommatidial arrangements (Fig. 3.14B, B'), the *hnt*^{peb} mutant retinas display disturbances in the stereotypical hexagonal arrangement, such as ommatidial fusion due to the absence of the lattice cells and bristle clustering. Interestingly, the recruitment of CCs and 1°s was also notably affected; most ommatidial CC clusters consisted of fewer than the normal four-cell cluster, and the number of recruited 1°s was highly variable, ranging from one to three (Fig. 3.15C, C').
This experiment revealed that the *hnt*^{peb} mutant phenotype includes a previously unreported defect in CC recruitment. Taken together, the above results fully support and add to the findings by Pickup et al (2002), and suggest that Hnt may be a critical factor in cell fate determinations during retinal development.

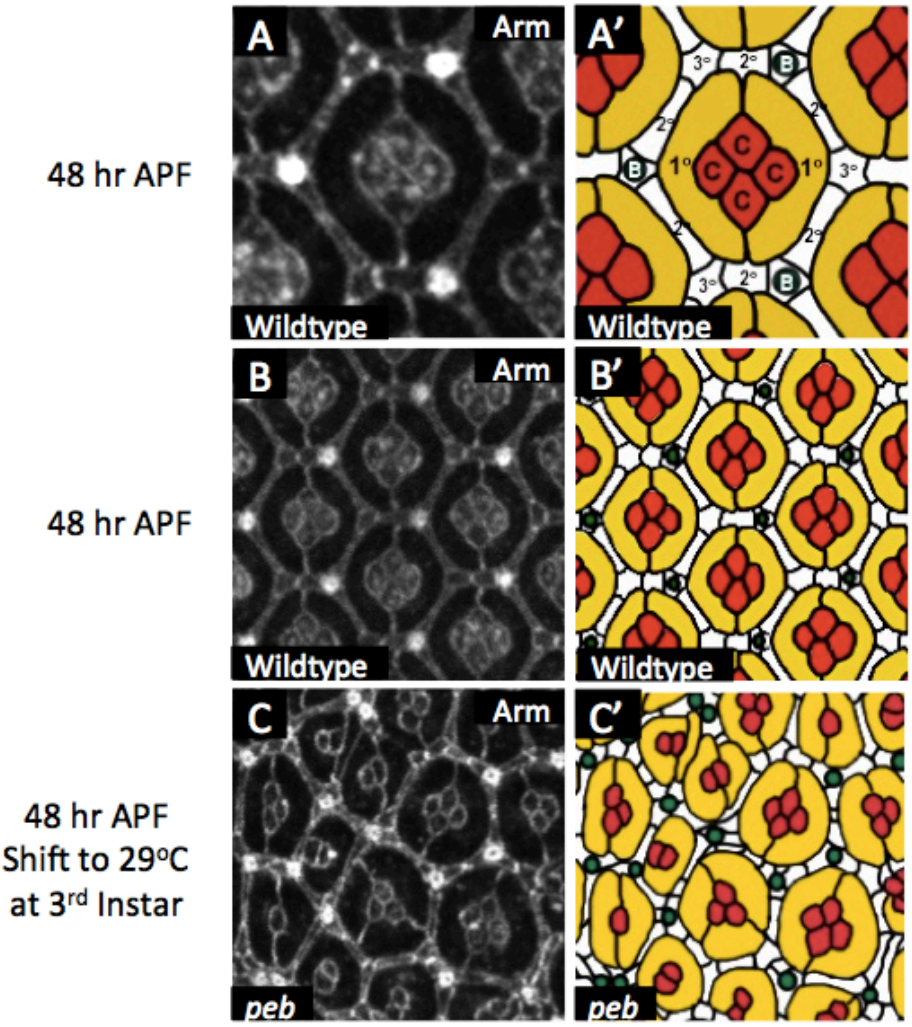

Figure 3.15 Hnt is required for proper recruitment and development of ommatidial cells
Pupal eyes 48 hr APF immunostained with anti-Armadillo showing organization of the retinal epithelium in wildtype (A, B) and in hnt^{peb} mutants (C). Confocal micrographs (A, B, C) and cartoon schematics for each (A', B', C') are shown. The apical surface of the eye of a wildtype ommatidium consists of four CCs (red), two 1°s (yellow), six 2°s (white), three 3°s (white), and three bristle cells (as shown in A'). A direct comparison of wildtype (B, B') and hnt^{peb} (*peb*) (C, C') mutant retinas at the same magnification shows a highly disorganized ommatidial structure in the mutant retinas, including a reduction in the number of CCs per ommatidium.

Chapter 4: Discussion

4.1 Regulation of *hnt* during *Drosophila* embryonic development

In this study, I addressed the regulation of embryonic Hnt expression through two major signaling pathways used reiteratively during development: N and EGFR signaling. In the developing SOP lineage, Hnt expression is found in the founder SOP prior to asymmetric cell division, but its expression becomes ultimately confined to the neurons (Pickup et al., 2002; Reeves and Posakony, 2005). *N* mutants disrupt the normal development of the SOP lineage, and result in a hypertrophic PNS. In this context, strong anti-Hnt staining was observed throughout the hypertrophic PNS, suggesting that embryonic Hnt expression in this tissue is not dependent on N signaling.

Additionally, in this study, the novel observation of *hnt* being a N-responsive gene was found in the context of embryonic hemocyte cells upon global expression of activated N in the embryo. In *Drosophila*, hematopoiesis occurs in two distinct phases (Meister and Lagueux, 2003). The first phase occurs during the second-half of embryogenesis, originating from the head mesoderm to give rise to the embryonic hemocytes. The second phase occurs in larval lymph glands, which are derived from the lateral mesoderm at the end of embryogenesis. Additional hemocytes originating from the larval lymph gland continue to mature throughout larval development (Meister and Lagueux, 2003; Tepass et al., 1994). It has been previously shown that *hnt* is a N-responsive gene in the context of the larval hemocyte lineage in the lymph gland (Terriente-Felix et al., 2013). However, whether the same response occurs in embryos is not known. As demonstrated in Section 3.1, it is possible that embryonic hemocytes, like their larval counterparts, share the same cellular response to activate *hnt* expression upon

activation of N. Overall, these results suggest that the ability of N signaling to activate Hnt expression is highly tissue-specific, and during embryogenesis, N-dependent Hnt expression appears to be confined to the embryonic hemocyte lineage. Previous analysis of N-dependent expression of Hnt in the larval lymph involved the construction of fluorescent protein reporters using the N-responsive elements from the *hnt* upstream regulatory sequence. I examined embryos from three different reporter lines (provided by Dr. Sarah Bray) but was unable to detect any embryonic expression (data not shown). Thus, at this time, it is not possible to definitively establish that Hnt is indeed a direct target of N signaling during embryogenesis.

Analysis of *hnt* mutant embryos revealed novel observations, in that *hnt* mutant phenotypes were found to display striking similarities to *egfr* mutant embryos, particularly in the developing PNS and oenocyte recruitment. In the developing PNS, *hnt* mutants displayed a reduction from five to three chordotonal organs and their associated neurons. Additionally, oenocyte recruitment was found to be severely impaired in *hnt* mutants. The recruited BO-positive cells in *hnt* mutants, which were reduced in number, generally appeared smaller than wildtype oenocytes and were dispersed throughout the embryo. In contrast, wildtype oenocytes are tightly clustered in the dorso-lateral region in embryonic abdominal hemisegments. The dispersal of the BO-positive cells in *hnt* mutants suggests a defect in cell adhesion, which could be required for proper clustering of the oenocytes. Interestingly, Hnt has been implicated in the regulation of cell adhesion and collective cell migration in the context of anterior follicle cells and associated border cells in the adult ovary (Melani et al., 2008). This apparent defect in cell adhesion warrants further investigation. Overall, however, the process of oenocyte recruitment is

well-established to depend on levels of EGFR signaling, further suggesting that EGFR signaling is impaired in *hnt* mutant embryos. My observations of defects in the recruitment of chordotonal organs and oenocytes represent new additions to the list of phenotypic similarities between *hnt* and *egfr* mutants. These include failure in germ band retraction and dorsal closure, and the maintenance of tracheal epithelial integrity (Cela and Llimargas, 2006; Clifford and Schüpbach, 1992; Shen et al., 2013).

A possible explanation for the extensive similarities between *hnt* and *egfr* mutant phenotypes could be that Hnt expression in many embryonic tissues is not dependent on N signaling, but rather, is dependent on EGFR signaling. A precedent for EGFR-dependent Hnt expression is found within the intestinal stem cells of the adult midgut (Baechler, 2014). It has been previously reported that Hnt expression remains "normal" in *egfr* mutants (Yip et al., 1997). My analysis of Hnt immunolocalization used fluorescence confocal microscopy rather than the immunohistochemical techniques and standard bright field microscopy that were used in the previous study. This more rigorous examination of Hnt immunolocalization in *egfr* mutant embryos revealed that Hnt expression was not entirely "normal". In addition to the obvious absence of oenocyte expression, the overall expression of Hnt in *egfr* mutant embryos appeared reduced. Whether or not this reduction is associated with defects in EGFR-dependent differentiation, or is possibly a consequence of *hnt* being a direct target of the EGFR signaling pathway remains uncertain. As mentioned above, EGFR signaling is pivotal in the formation of chordotonal organs, recruitment of oenocytes, and invagination, primary branching, and maintenance of the epithelial integrity within the tracheal system (Cela and Llimargas, 2006; Lage and Jarman, 1999; Llimargas and Casanova, 1999; Rusten et

al., 2001). Each of these examples is associated with strong Hnt expression. My observations of Hnt immunolocalization lead me to speculate that the expression of Hnt does not absolutely require EGFR signaling, but the possibility that an upregulation of Hnt in some tissues could be EGFR-dependent.

Interestingly, I found that overexpression of two components of the EGFR signaling pathway, the active ligand sSpi or activated Ras, led to an expansion of Hnt expression in the dorso-lateral region of the embryo. In previous studies, supernumerary oenocyte recruitment was observed upon overexpression of sSpi (Elstob et al., 2001), and thus, it can be speculated that the expansion of Hnt expression via sSpi overexpression is most likely an indirect effect of supernumerary oenocyte recruitment. In addition, although overexpression of Ras has not been directly associated with additional oenocyte recruitment, the expansion of Hnt expression in the dorso-lateral region of the embryo, as well as the cellular morphology of these cells, suggested that this response may be indirect through additional oenocyte recruitment. Overall, the above results suggest that the dependence and responsiveness of *hnt* to N or EGFR signaling seems to be highly context-specific.

Ultimately, the activation of the EGFR/Ras/MAPK pathway results in the phosphorylation of the transcriptional regulators, Pointed and Yan. In general, Pointed is activated by MAPK and promotes the transcription of numerous EGFR target genes. On the other hand, Yan normally functions as a negative regulator of EGFR target genes, and its activity is inactivated by MAPK. Interestingly, previous genetic interaction studies have shown that the temperature-sensitive hypomorphic phenotype of hnt^{peb} is suppressed in a dosage-sensitive manner by loss of function *yan* alleles (Wilk et al., 2004). This

genetic interaction is consistent with the possibility that Hnt is a direct target of EGFR signaling. The activation of Hnt expression by the Pnt transcription factor, however, has not been addressed either in the literature or in our lab. In addition, an analysis of the extensive upstream regulatory region of *hnt* for putative Pnt/Yan (ETS transcription factor) binding sites has not been performed. The suppression of hnt^{peb} by Yan, however, is also consistent with the possibility of Hnt negatively regulating Yan without itself being a target of the EGFR signaling pathway (see future directions).

4.2 Hnt-dependent embryonic DPax2 induction requires EGFR signaling

The examination of effects on DPax2 reporter expression following Hnt overexpression indicated that a 3.1 kb region which lies within the *sv* enhancer is responsive to Hnt overexpression. The *sv* enhancer has been described as a bristle-specific enhancer, and given that bristles are a component of the PNS, in addition to the finding that Hnt overexpression resulted in ectopic DPax2 throughout what appeared to be an expansion of the embryonic PNS, it is tempting to speculate that Hnt's effect on DPax2 expression is PNS-specific. However, embryonic DPax2 induction by Hnt overexpression was also found to occur within the embryonic salivary gland. Overall, the response to Hnt overexpression was not only PNS-specific, but displays an apparent tissue-specific threshold-effect. The embryonic salivary gland likely displays the lowest threshold for Hnt-dependent ectopic DPax2 expression. Based on the model for the induction of DPax2 expression within the pupal retina, where DPax2 expression requires inputs from both the N and EGFR signaling pathways, a similar analysis was performed in the embryo. Here it was found that the induction of DPax2 expression by Hnt overexpression is indirect, as this effect was sensitive to the dosage of EGFR, and was completely abolished in the absence of EGFR. Furthermore, activation of EGFR signaling in the embryo was found to also expand DPax2 expression, however, simultaneous overexpression of activated Ras and EP55 revealed that Hnt creates an additive effect to increase the expansion of DPax2 expression.

These results not only confirm that the upregulation of DPax2 expression via Hnt overexpression is dependent on EGFR signaling, but also reveal the capacity of EGFR signaling to activate DPax2 expression in the embryo. The results of this study suggest

that increased EGFR signaling is sufficient to induce an expansion of the domain of DPax2 expression, regardless of the presence of Hnt. In addition, the expansion of DPax2 expression displayed an additive effect upon simultaneous expression of activated Ras and Hnt. This is consistent with the interpretation that Hnt amplifies the EGFR signaling pathway to stimulate EGFR-sensitive DPax2 expression. Such relationship between EGFR signaling and Hnt is not unprecedented. In mammals, the Hnt homolog, RREB1, has been described to potentiate levels of Ras/MAPK signaling. The mechanism has been suggested to involve the direct binding of RREB1, which results in the repression of the microRNAs genes, *miR-143 or miR-145*. These microRNA genes are proposed to function as negative feedback regulators of the EGFR signaling pathway (Kent et al., 2010; Saj and Lai, 2011). Since the function and binding sequences of Hnt and RREB1 have been suggested to be conserved (Ming et al., 2014), Hnt may increase DPax2 expression using a similar mechanism to potentiate EGFR signaling. Interestingly, in *Drosophila*, one of the positive-feedback regulators of the EGFR signaling pathway is the microRNA gene, *miR-7*. In this case, however, *miR-7* targets the negative regulator Yan, promoting EGFR pathway activation and any possible repression of this target gene by Hnt would have a dampening effect (Li and Carthew, 2005). At the present time, no microRNA genes have been identified to function as negative-feedback regulators of the EGFR signaling pathway, but such a category of genes would be strong candidates as targets of Hnt, should the mammalian mechanism prove to be conserved.

4.3 DPax2 is responsive to Hnt misexpression in the pupal eye

The *DPax2* gene has been well characterized and mutants disrupting eye development were originally isolated as alleles of the gene *sparkling* (*spa*), while mutants disrupting bristle development were isolated as alleles of the gene *shaven* (*sv*) (Fu and Noll, 1997; Fu et al., 1998; Hochman, 1971; Kavaler et al., 1999). It was eventually established that the DPax2 gene behaves as a complex locus and that *spa* and *sv* alleles disrupt two distinct regulatory regions required for eye and bristle development, respectively (Fu et al., 1998). Curiously, despite directed efforts, a null DPax2 allele has not been isolated. The intronic regulatory region associated with *spa* alleles has been studied exhaustively in association with DPax2 expression in the CCs of the developing pupal retina (Flores et al., 2000; Swanson et al., 2010; Swanson et al., 2011). The upstream regulatory region associated with *sv* alleles has been characterized with respect to expression in the microchaetae SOP lineage, but has not been analyzed with respect to CC expression (Johnson et al., 2011). While the *spa* enhancer is well described as activating CC-specific expression of DPax2, I found that the upstream *sv* enhancer region, used to drive the $DPax2^{B}$ reporters, is also associated with CC expression. Curiously, the *spa* enhancer drives expression in all four CCs, while DPax2B reporters show prominent expression in only one or two CCs, depending on the developmental stage. It has been previously shown that the developing CCs have four distinct subtypes (anterior, posterior, polar, and equatorial) that show differential DPax2 expression, in which the anterior and posterior show higher DPax2 expression (Charlton-Perkins et al., 2011). Based on my observations of the expression of the $DPax2^{B}$ reporter, it is likely that this non-equivalent expression

pattern within the four CCs results from DPax2 expression associated with the upstream *sv* enhancer.

In the experiments in which Hnt overexpression was induced 24 hr APF, ectopic DPax2 expression was observed using the DPax2^{B} reporter, demonstrating that, as is the case in the embryo, Hnt overexpression likely acts through the *sv* enhancer. Interestingly, in these experiments, ectopic DPax2 expression was most prominent in cells other than the CCs, and no supernumerary CCs were detected. In several studies, CC number has been directly associated with the activity of the EGFR signaling pathway, where reduced EGFR signaling consistently results in less than four CCs per ommatidium, whereas increased EGFR signaling induces supernumerary CCs (Domínguez et al., 1998; Freeman, 1996; Wech and Nagel, 2005). In a different experiment in which Hnt overexpression was induced at an earlier developmental stage using the *GMR-GAL4* driver, supernumerary CCs were plentiful. This result suggests that Hnt overexpression in the pupal eye can also amplify EGFR signaling, but that there is a window of competence for this effect. Significantly, supernumerary CCs were not associated with *GMR-GAL4* driven expression of GFP-HNT, indicating that this induction occurred non-autonomously. Overall, this study revealed the responsiveness of DPax2 in the pupal eye to Hnt overexpression through the *sv* enhancer, and suggests that the sensitivity of DPax2's response is variable depending on the developmental timing of the pupal retina. While these experiments using the pupal eye are consistent with observations made in the embryo, the EGFR-dependence of DPax2 expression resulting from Hnt overexpression has yet to be definitively established.

4.4 Hnt and its possible relationship to EGFR signaling during development

Previous analysis on *hnt*^{peb} mutants has shown many R cell abnormalities, mainly missing outer R cells, and defects in establishing planar polarity (Pickup et al., 2002). This work, however, did not include analysis of the pupal retinal epithelium 48 hr APF, at which time, I found *hnt*^{peb} to display striking defects in CC recruitment. The *hnt*^{peb} mutation, which has been described as a temperature sensitive allele, has not been analyzed molecularly, and the consequences of shifting to the restrictive temperature of 29°C is largely unknown. That is, it is presently unknown if the restrictive temperature reduces the expression of *hnt*^{peb}, or if the Hnt^{peb} protein is destabilized. Regardless of the mechanism, reduced CC induction at the restrictive temperature clearly shows that *hnt*^{peb} functions non-autonomously since Hnt is not expressed in CCs. Numerous studies reported in the literature link CC induction with EGFR signaling (Behan et al., 2002; Domínguez et al., 1998; Freeman, 1996; Wech and Nagel, 2005; Yogev et al., 2008). Overall, the striking effect of both *hnt* loss of function as well as overexpression on the recruitment of CCs strongly suggests that Hnt functions in the pupal eye to modulate EGFR signaling. The apparent non-autonomy of Hnt with respect to CC induction suggests that if Hnt is, in fact, modulating EGFR signaling, it could be doing so by influencing the production of activated EGFR ligands.

During eye development, EGFR signaling is complex and dynamic. In wildtype retinas, EGFR signaling is used in several waves throughout eye morphogenesis. The first three waves occur within the third instar larval eye disc. The initial wave of EGFR signaling establishes proper R8 spacing, and the subsequent organization of the proneural clusters which ultimately determines the organization of the hexagonal array of

ommatidia in the adult retina (Baonza et al., 2001; Domínguez et al., 1998). The second wave of EGFR signaling is required for the recruitment of R1-R7, which surround R8, where excess signal from R8 can recruit additional R cells(Freeman, 1996). The third wave is responsible for the regulation of cell proliferation in the developing larval eye disc, where excess signal promotes cell proliferation. It is important to note that a temporal gradient is present in the developing retina, in which the cells of the developing retina have a window of competence to differentiate and be receptive to various signals. With each successive wave of the EGFR signal, different cell types that develop at the respective time frames are competent to the signal, and therefore, studies directed to misexpress identical components of the EGFR signaling pathways will have different outcomes depending on the timing of the misexpression (Domínguez et al., 1998). The fourth wave occurs after R cell determination in the larval eye disc, and continues into pupal development, where the activation of EGFR signaling, in combination with other regulatory factors, determines the cell fate of CCs/1°s/2°s/3°s at distinct stages (Domínguez et al., 1998; Flores et al., 2000; Freeman, 1996; Miller and Cagan, 1998; Wech and Nagel, 2005; Wildonger et al., 2005). Lastly, the final wave of EGFR signaling occurs approximately 22 hours APF, when PCD occurs to eliminate excess lattice cells (Miller and Cagan, 1998). EGFR signaling, at this time point, serves as a cell survival signal, where in combination with N signaling, it regulates the elimination of approximately 2000 lattice cells via PCD, ultimately resulting in the exquisitely precise hexagonal arrangement of the ommatidia (Bergmann et al., 2002; Miller and Cagan, 1998; Wech and Nagel, 2005)

My observations of three different experiments performed in the pupal retina, these being: 1) Hnt overexpression 24 APF (GAL80^{ts} + *GMR-GAL4>UAS-GFP-HNT$_{(II)}$* = late/strong); 2) Hnt overexpression (*GMR-GAL4>UAS-GFP-HNT^{J27}* = early/weak); and 3) *hnt^{peb}* mutant analysis (conditional hypomorph), are all consistent with the possibility that Hnt functions to modulate EGFR signaling. Each of these experiments resulted in different phenotypes, and these differences can be explained by the sensitivity of the developing pupal eye to the levels and timing of EGFR activation. In the first experiment, there was no defect in CC recruitment, while the interstitial lattice was greatly perturbed. The second experiment resulted in supernumerary CCs, while the third experiment resulted in reduced CCs. The observations of the first two experiments are likely best explained by the different times at which Hnt overexpression was induced, whereas the observations in the third (*hnt^{peb}*) experiment likely reflect reduced levels of EGFR signaling. The latter possibility can be confirmed by Hnt immunostaining combined with *hnt^{peb}* clonal analysis (see Future directions)

However, as discussed previously, *hnt* is a bona-fide N responsive gene in several contexts (Housden et al., 2013; Krejci et al., 2009; Terriente-Felix et al., 2013), and therefore, the possibility of Hnt acting to mediate the interplay of N and EGFR signaling, both of which are required for proper eye morphogenesis, remains. Overall, my observations from both the embryo and the pupal retina strongly suggest an overarching theme of Hnt acting to potentiate levels of the EGFR signaling pathway.

Chapter 5: Future Directions

5.1 Addressing the role of Hnt in the EGFR signaling pathway

The presented data suggests a strong link between Hnt and the EGFR signaling pathway, where Hnt may be involved in the potentiation of the levels of EGFR signaling. Preliminary results from both the embryonic context and the pupal retina are suggestive of this link, however, the pupal retina serves as a better tissue to work with due to the wealth of information available regarding this tissue-context. In addition, embryos consist of all differentiating tissue types, and therefore, may not be a specific method for testing such detailed responses. As mentioned in Section 4.1, hnt^{peb} mutation was previously observed to genetically interact with Yan, a transcriptional repressor of the EGFR signaling pathway (Wilk et al., 2004). If Hnt modulates levels of EGFR signaling by interacting with Yan, speculatively, Hnt would act as a negative regulator of Yan to repress its functions, ultimately allowing for increased output of EGFR signaling. However, similar to mammals, the possibility of Hnt binding to microRNA genes remains. Ultimately, it would be beneficial to identify potential target genes of Hnt through high-throughput techniques such as chromatin immunoprecipitation-sequencing (ChIP-Seq).

Additionally, it would be beneficial to determine whether *hnt* itself could be a target of the EGFR signaling pathway. This can be achieved through the identification of possible ETS-transcription factor DNA binding domains in the upstream regulatory region of *hnt*, and testing the interaction between the putative ETS-protein binding sequence and Pnt/Yan. Alternatively, Hnt may be a direct target of MAPK itself, and phosphorylation of Hnt by MAPK may also lead to differential protein activity. The

phosphorylation of Hnt would be consistent with the activity of the mammalian homolog, RREB1, where RREB1 is a direct target of MAPK, and serves as a transcriptional repressor to bind to microRNA genes, ultimately leading to an upregulation of Ras/MAPK signaling (Saj and Lai, 2011). Additionally, a phosphoproteome analysis in *Drosophila* embryos has revealed eleven distinct phosphorylation sites within the Hnt protein (Zhai et al., 2008), two of which contain conserved MAPK-consensus phosphorylation sites. Therefore, it would be of great interest to determine whether Hnt can be phosphorylated via MAPK, which would be most efficiently done using *in vitro* techniques to ultimately perform mobility shift assays to visualize a shift in the Hnt protein upon introduction to a concentrate of activated MAPK.

5.2 Clonal analysis in the pupal eye

It has been clearly established that in both the embryo and the pupal eye, DPax2 is responsive to Hnt through the *sv* enhancer. Whether this response is associated with the EGFR signaling pathway was not established in the pupal eye, due to *egfr* mutants being embryonic lethal. Generating *egfr* mutant clones in the pupal eye overexpressing Hnt would serve as a great technique to establish whether this response from DPax2 upon Hnt overexpression is EGFR-dependent, and would provide a direct comparison between the tissue area that do not contain the clonal patches. Additionally, generating clonal patches of GFP-HNT^{J27} overexpression in the pupal eye would address whether the induction of supernumerary CCs is indeed a non-autonomous response. Finally, whether *hnt*^{peb} results in reduced EGFR signaling can be addressed by generating clones in the pupal eye then performing an anti-pMAPK immunostaining to compare relative levels of activated MAPK levels in *hnt*^{peb} directly with a wildtype internal control tissue.

References

Artavanis-Tsakonas, S., Rand, M. D. and Lake, R. J. (1999). Notch Signaling: Cell Fate Control and Signal Integration in Development. *Science* **284**, 770-776.

Baechler, B. (2014). Investigation of the role of Hindsight in the development of the *Drosophila* midgut. 1–92.

Baonza, A., Casci, T. and Freeman, M. (2001). A primary role for the epidermal growth factor receptor in ommatidial spacing in the Drosophila eye. *Curr. Biol.* **11**, 396–404.

Behan, K. J., Nichols, C. D., Cheung, T. L., Farlow, A., Hogan, B. M., Batterham, P. and Pollock, J. A. (2002). Yan regulates Lozenge during Drosophila eye development. *Dev. Genes Evol.* **212**, 267–276.

Bergmann, A., Tugentman, M., Shilo, B.-Z. and Steller, H. (2002). Regulation of cell number by MAPK-dependent control of apoptosis: a mechanism for trophic survival signaling. *Developmental Cell* **2**, 159–170.

Brand, A. H. and Perrimon, N. (1993). Targeted gene expression as a means of altering cell fates and generating dominant phenotypes. *Development* **118**, 401–415.

Bray, S. J. (2006). Notch signalling: a simple pathway becomes complex. *Nat. Rev. Mol. Cell Biol.* **7**, 678–689.

Brewster, R. and Bodmer, R. (1995). Origin and specification of type II sensory neurons in Drosophila. *Development* **121**, 2923–2936.

Bufflin, E. and Gho, M. (2010). Laser Microdissection of Sensory Organ Precursor Cells of Drosophila Microchaetes. *PLoS ONE* **5**, 1–9.

Cagan, R. L. and Ready, D. F. (1989). The Emergence of Order in the *Drosophila* Pupal Retina. *Developmental Biology* **136**, 346–362.

Carlson, J. R. (1996). Olfaction in Drosophila: from odor to behavior. *Trends Genet.* **12**, 175–180.

Cela, C. and Llimargas, M. (2006). Egfr is essential for maintaining epithelial integrity during tracheal remodelling in Drosophila. *Development* **133**, 3115–3125.

Charlton-Perkins, M., Whitaker, S. L., Fei, Y., Xie, B., Li-Kroeger, D., Gebelein, B. and Cook, T. (2011). Prospero and Pax2 combinatorially control neural cell fate decisions by modulating Ras- and Notch-dependent signaling. *Neural Dev* **6**, 20.

Clifford, R. and Schüpbach, T. (1992). The torpedo (DER) receptor tyrosine kinase is required at multiple times during Drosophila embryogenesis. *Development* **115**, 853–

872.

Cubas, P., de Celis, J. F., Campuzano, S. and Modolell, J. (1991). Proneural clusters of achaete-scute expression and the generation of sensory organs in the *Drosophila* imaginal wing disc. *Genes & Development* **5**, 996-1008.

De Celis, J. F., Marí-Beffa, M. and García-Bellido, A. (1991). Cell-autonomous role of Notch, an epidermal growth factor homologue, in sensory organ differentiation in Drosophila. *Proc. Natl. Acad. Sci. U.S.A.* **88**, 632–636.

Diaz-Benjumea, F. J. and Hafen, E. (1994). The sevenless signaling cassette mediates Drosophila EGF receptor function during epidermal development. *Development* **120**, 569–578.

Domínguez, M., Wasserman, J. D. and Freeman, M. (1998). Multiple functions of the EGF receptor in Drosophila eye development. *Curr. Biol.* **8**, 1039–1048.

Du, O. Y. (2013). Identification of genes regulated by the Drosophila transcription factor Hindsight. 1–158.

Duffy, J. B. (2002). GAL4 system in *Drosophila*: A fly geneticist's swiss army knife. *Genesis* **34**, 1–15.

Elstob, P. R., Brodu, V. and Gould, A. P. (2001). *spalt*-dependent switching between two cell fates that are induced by the Drosophila EGF receptor. *Development* **128**, 723–732.

Flores, G. V., Duan, H., Yan, H., Nagaraj, R., Fu, W., Zou, Y., Noll, M. and Banerjee, U. (2000). Combinatorial signaling in the specification of unique cell fates. *Cell* **103**, 75–85.

Franc, N. C., Dimarcq, J. L., Lagueux, M., Hoffmann, J. and Ezekowitz, R. A. (1996). Croquemort, a novel *Drosophila* hemocyte/macrophage receptor that recognizes apoptotic cells. *Immunity* **4**, 431–443.

Freeman, M. (1996). Reiterative use of the EGF receptor triggers differentiation of all cell types in the *Drosophila* eye. *Cell* **87**, 651–660.

Fu, W. and Noll, M. (1997). The Pax2 homolog sparkling is required for development of cone and pigment cells in the Drosophila eye. *Genes Dev.* **11**, 2066–2078.

Fu, W., Duan, H., Frei, E. and Noll, M. (1998). *shaven* and *sparkling* are mutations in separate enhancers of the *Drosophila* Pax2 homolog. *Development* **125**, 2943–2950.

Gabay, L., Scholz, H., Golembo, M., Klaes, A., Shilo, B. Z. and Klämbt, C. (1996). EGF receptor signaling induces pointed P1 transcription and inactivates Yan protein in the Drosophila embryonic ventral ectoderm. *Development* **122**, 3355–3362.

Gould, A. P., Elstob, P. R. and Brodu, V. (2001). Insect oenocytes: a model system for studying cell-fate specification by Hox genes. *J. Anat.* **199**, 25–33.

Hartenstein, A. Y., Rugendorff, A., Tepass, U. and Hartenstein, V. (1992). The function of the neurogenic genes during epithelial development in the *Drosophila* embryo. *Development* **116**, 1203–1220.

Hochman, B. (1971). Analysis of chromosome 4 in Drosophila melanogaster. II. Ethyl methanesulfonate induced lethals. *Genetics* **67**, 235–252.

Housden, B. E., Fu, A. Q., Krejci, A., Bernard, F., Fischer, B., Tavaré, S., Russell, S. and Bray, S. J. (2013). Transcriptional dynamics elicited by a short pulse of notch activation involves feed-forward regulation by E(spl)/Hes genes. *PLoS Genet.* **9**, e1003162.

Jarman, A. P., Sun, Y., Jan, L. Y. and Jan, Y. N. (1995). Role of the proneural gene, atonal, in formation of Drosophila chordotonal organs and photoreceptors. *Development* **121**, 2019–2030.

Johnson, S. A., Harmon, K. J., Smiley, S. G., Still, F. M. and Kavaler, J. (2011). Discrete Regulatory Regions Control Early and Late Expression of *D-Pax2* During External Sensory Organ Development. *Dev. Dyn.* **240**, 1769–1778.

Kavaler, J., Fu, W., Duan, H., Noll, M. and Posakony, J. W. (1999). An essential role for the *Drosophila* Pax2 homolog in the differentiation of adult sensory organs. *Development* **126**, 2261–2272.

Kent, O. A., Chivukula, R. R., Mullendore, M., Wentzel, E. A., Feldmann, G., Lee, K. H., Liu, S., Leach, S. D., Maitra, A. and Mendell, J. T. (2010). Repression of the miR-143/145 cluster by oncogenic Ras initiates a tumor-promoting feed-forward pathway. *Genes Dev.* **24**, 2754–2759.

Klämbt, C. (1993). The *Drosophila* gene *pointed* encodes two ETS-like proteins which are involved in the development of the midline glial cells. *Development* **117**, 163–176.

Kopan, R. and Ilagan, M. (2009). ScienceDirect.com - Cell - The Canonical Notch Signaling Pathway: Unfolding the Activation Mechanism. *Cell*.

Krejci, A., Bernard, F., Housden, B. E., Collins, S. and Bray, S. J. (2009). Direct Response to Notch Activation: Signaling Crosstalk and Incoherent Logic. *Science Signaling* **2**, ra1–ra1.

Lage, P., Jan, Y. N. and Jarman, A. P. (1997). Requirement for EGF receptor signalling in neural recruitment during formation of Drosophila chordotonal sense organ clusters. *Curr. Biol.* **7**, 166–175.

Lage, P. and Jarman, A. P. (1999). Antagonism of EGFR and Notch signaling in the

reiterative recruitment of Drosophila adult chordotonal sense organ precursors. *Development* **126**, 3149–3157.

Lage, P. I., Powell, L. M., Prentice, D. R. A., McLaughlin, P. and Jarman, A. P. (2004). EGF receptor signaling triggers recruitment of Drosophila sense organ precursors by stimulating proneural gene autoregulation. *Developmental Cell* **7**, 687–696.

Lai, E. C. and Orgogozo, V. (2004). A hidden program in Drosophila peripheral neurogenesis revealed: fundamental principles underlying sensory organ diversity. *Developmental Biology* **269**, 1–17.

Lamka, M. L. and Lipshitz, H. D. (1999). Role of the amnioserosa in germ band retraction of the Drosophila melanogaster embryo. *Developmental Biology* **214**, 102–112.

Li, X. and Carthew, R. W. (2005). A microRNA mediates EGF receptor signaling and promotes photoreceptor differentiation in the Drosophila eye. *Cell* **123**, 1267–1277.

Liu, H., Hew, H. C., Lu, Z.-G., Yamaguchi, T., Miki, Y. and Yoshida, K. (2009). DNA damage signalling recruits RREB-1 to the p53 tumour suppressor promoter. *Biochem. J.* **422**, 543–551.

Llimargas, M. and Casanova, J. (1999). EGF signaling regulates cell invagination as well as cell migration during formation of tracheal system in *Drosophila*. *Dev. Genes Evol.* **209**, 174–179.

Louvi, A. and Artavanis-Tsakonas, S. (2006). Notch signaling in vertebrate neural development. *Nat. Rev. Neurosci.* **7**, 93–102.

Meister, M. and Lagueux, M. (2003). *Drosophila* blood cells. *Cell. Microbiol.* **5**, 573–580.

Melani, M., Simpson, K. J., Brugge, J. S. and Montell, D. (2008). Regulation of cell adhesion and collective cell migration by *hindsight* and its human homolog RREB1. *Curr. Biol.* **18**, 532–537.

Miller, D. T. and Cagan, R. L. (1998). Local induction of patterning and programmed cell death in the developing *Drosophila* retina. *Development* **125**, 2327–2335.

Milon, B. C., Agyapong, A., Bautista, R., Costello, L. C. and Franklin, R. B. (2010). Ras responsive element binding protein-1 (RREB-1) down-regulates hZIP1 expression in prostate cancer cells. *Prostate* **70**, 288–296.

Ming, L., Wilk, R., Reed, B. H. and Lipshitz, H. D. (2014). *Drosophila* Hindsight and mammalian RREB-1 are evolutionarily conserved DNA-binding transcriptional attenuators. *Differentiation* **86**, 159-170.

O'Neill, E. M., Rebay, I., Tjian, R. and Rubin, G. M. (1994). The activities of two Ets-related transcription factors required for Drosophila eye development are modulated by the Ras/MAPK pathway. *Cell* **78**, 137–147.

Okabe, M. and Okano, H. (1997). Two-step induction of chordotonal organ precursors in Drosophila embryogenesis. *Development*.

Oliva, C. and Sierralta, J. (2010). Regulation of axonal development by the nuclear protein *hindsight* (*pebbled*) in the *Drosophila* visual system. *Developmental Biology* **344**, 911–921.

Pickup, A. T., Lamka, M. L., Sun, Q., Yip, M. L. R. and Lipshitz, H. D. (2002). Control of photoreceptor cell morphology, planar polarity and epithelial integrity during Drosophila eye development. *Development* **129**, 2247–2258.

Pickup, A. T., Ming, L. and Lipshitz, H. D. (2009). Hindsight modulates Delta expression during Drosophila cone cell induction. *Development* **136**, 975–982.

Ready, D. F., Hanson, T. E. and Benzer, S. (1976). Development of the *Drosophila* retina, a neurocrystalline lattice. *Developmental Biology* **53**, 217–240.

Reed, B. H., McMillan, S. C. and Chaudhary, R. (2009). The preparation of Drosophila embryos for live-imaging using the hanging drop protocol. *J Vis Exp*.

Reed, B. H., Wilk, R. and Lipshitz, H. D. (2001). Downregulation of Jun kinase signaling in the amnioserosa is essential for dorsal closure of the Drosophila embryo. *Curr. Biol.* **11**, 1098–1108.

Reeves, N. and Posakony, J. W. (2005). Genetic Programs Activated by Proneural Proteins in the Developing Drosophila PNS. *Developmental Cell* **8**, 413–425.

Rusten, T. E., Cantera, R., Urban, J., Technau, G., Kafatos, F. C. and Barrio, R. (2001). Spalt modifies EGFR-mediated induction of chordotonal precursors in the embryonic PNS of Drosophila promoting the development of oenocytes. *Development* **128**, 711–722.

Rutledge, B. J., Zhang, K., Bier, E., Jan, Y. N. and Perrimon, N. (1992). The Drosophila *spitz* gene encodes a putative EGF-like growth factor involved in dorsal-ventral axis formation and neurogenesis. *Genes Dev.* **6**, 1503–1517.

Saj, A. and Lai, E. C. (2011). Control of microRNA biogenesis and transcription by cell signaling pathways. *Current Opinion in Genetics & Development* **21**, 504–510.

Schweitzer, R., Shaharabany, M., Seger, R. and Shilo, B. Z. (1995). Secreted Spitz triggers the DER signaling pathway and is a limiting component in embryonic ventral ectoderm determination. *Genes Dev.* **9**, 1518–1529.

Shen, W., Chen, X., Cormier, O., Cheng, D. C.-P., Reed, B. and Harden, N. (2013).

Modulation of morphogenesis by Egfr during dorsal closure in Drosophila. *PLoS ONE* **8**, e60180.

Shilo, B.-Z. (2005). Regulating the dynamics of EGF receptor signaling in space and time. *Development* **132**, 4017–4027.

Sun, J. and Deng, W.-M. (2007). Hindsight mediates the role of notch in suppressing hedgehog signaling and cell proliferation. *Developmental Cell* **12**, 431–442.

Sundaram, M. V. (2005). The love-hate relationship between Ras and Notch. *Genes Dev.* **19**, 1825–1839.

Swanson, C. I., Evans, N. C. and Barolo, S. (2010). Structural rules and complex regulatory circuitry constrain expression of a Notch- and EGFR-regulated eye enhancer. *Developmental Cell* **18**, 359–370.

Swanson, C. I., Schwimmer, D. B. and Barolo, S. (2011). Rapid evolutionary rewiring of a structurally constrained eye enhancer. *Curr. Biol.* **21**, 1186–1196.

Tepass, U., Fessler, L. I., Aziz, A. and Hartenstein, V. (1994). Embryonic origin of hemocytes and their relationship to cell death in Drosophila. *Development* **120**, 1829–1837.

Terriente-Felix, A., Li, J., Collins, S., Mulligan, A., Reekie, I., Bernard, F., Krejci, A. and Bray, S. (2013). Notch cooperates with Lozenge/Runx to lock haemocytes into a differentiation programme. *Development* **140**, 926-937.

Thiagalingam, A., Lengauer, C., Baylin, S. B. and Nelkin, B. D. (1997). RREB1, a ras responsive element binding protein, maps to human chromosome 6p25. *Genomics* **45**, 630–632.

Voas, M. G. and Rebay, I. (2003). Signal integration during development: Insights from the *Drosophila* eye. *Dev. Dyn.* **229**, 162–175.

Wech, I. and Nagel, A. C. (2005). Mutations in rugose promote cell type-specific apoptosis in the *Drosophila* eye. *Cell Death Differ.* **12**, 145–152.

Wildonger, J., Sosinsky, A., Honig, B. and Mann, R. S. (2005). Lozenge directly activates *argos* and *klumpfuss* to regulate programmed cell death. *Genes Dev.* **19**, 1034–1039.

Wilk, R., Pickup, A. T., Hamilton, J. K., Reed, B. H. and Lipshitz, H. D. (2004). Dose-sensitive autosomal modifiers identify candidate genes for tissue autonomous and tissue nonautonomous regulation by the *Drosophila* nuclear zinc-finger protein, *hindsight*. *Genetics* **168**, 281–300.

Wilk, R., Reed, B. H., Tepass, U. and Lipshitz, H. D. (2000). The *hindsight* gene is required for epithelial maintenance and differentiation of the tracheal system in

Drosophila. *Developmental Biology* **219**, 183–196.

Wolff, T. and Ready, D. F. (1991). The beginning of pattern formation in the *Drosophila* compound eye: the morphogenetic furrow and the second mitotic wave. *Development* **113**, 841–850.

Yang, L. and Baker, N. E. (2001). Role of the EGFR/Ras/Raf pathway in specification of photoreceptor cells in the Drosophila retina. *Development* **128**, 1183–1191.

Yip, M. L. R., Lamka, M. L. and Lipshitz, H. D. (1997). Control of germ-band retraction in Drosophila by the zinc-finger protein HINDSIGHT. *Development* **124**, 2129–2141.

Yogev, S., Schejter, E. D. and Shilo, B.-Z. (2008). Drosophila EGFR signalling is modulated by differential compartmentalization of Rhomboid intramembrane proteases. *EMBO J.* **27**, 1219–1230.

Zeidler, M. P., Tan, C., Bellaiche, Y., Cherry, S., Häder, S., Gayko, U. and Perrimon, N. (2004). Temperature-sensitive control of protein activity by conditionally splicing inteins. *Nat. Biotechnol.* **22**, 871–876.

Zhai, B., Villén, J., Beausoleil, S. A., Mintseris, J. and Gygi, S. P. (2008). Phosphoproteome analysis of *Drosophila* melanogaster embryos. *J. Proteome Res.* **7**, 1675–1682.

Zhang, L., Zhao, J. and Edenberg, H. J. (1999). A human Raf-responsive zinc-finger protein that binds to divergent sequences. *Nucleic Acids Res.* **27**, 2947–2956.

Zhang, S., Qian, X., Redman, C., Bliskovski, V., Ramsay, E. S., Lowy, D. R. and Mock, B. A. (2003). p16 INK4a gene promoter variation and differential binding of a repressor, the ras-responsive zinc-finger transcription factor, RREB. *Oncogene* **22**, 2285–2295.

Appendix A: Stocks and Crossing Schemes

Table A1. Genetic Stocks

Genotype	Source
yw hnt^{XE81}FRT19A/FM7	Bloomington Drosophila Stock Center
N^{55e11}/FM7c	Bloomington Drosophila Stock Center
yw; UAS-N^{intra}/CyO	Bloomington Drosophila Stock Center
Df(1)rb^{1}/FM7	H. Lipshitz
yw; BO-GAL4	A. Gould
w; UAS-GFP^{nls14}	Bloomington
w;; DPax2^{A1}-GFP	J. Kavaler
w;; DPax2^{B1}-GFP	J. Kavaler
w;; DPax2^{B1}dsRed	J. Kavaler
w; DPax2^{B2}-GFP	J. Kavaler
w; DPax2^{B2}dsRed	J. Kavaler
w;; DPax2^{C1}-GFP	J. Kavaler
w;; DPax2^{C4}-GFP	J. Kavaler
w;; DPax2^{D1}-GFP	J. Kavaler
w;; DPax2^{D7}-GFP	J. Kavaler
w; Egfr^{f2} /CyO	Bloomington Drosophila Stock Center
w; UbiDECadGFP + Egfr^{1a15}/CyO, TwiG	Reed Lab Stock Collection
w; Gla/CyO	Reed Lab Stock Collection
w; dp^{1a15}UbiDECadGFPEgfr^{1a15}/CyO	Bloomington Drosophila Stock Center
w;; daughterless-GAL4 (daGAL4)	Bloomington Drosophila Stock Center
w peb^{EP55}	Bloomington Drosophila Stock Center
yw EP55 FRT19A ;; DPax2^{B1}dsRed	Reed Lab Stock Collection
w;; UAS-sSpi/TM6 [Gal80]	Bloomington Drosophila Stock Center
w;; UAS-Ras85D^{V12}	Bloomington Drosophila Stock Center
UAS-Ras85D^{N17} (on X)	Bloomington Drosophila Stock Center
w; UAS-GFP-HNT$_{(II)}$	H. Lipshitz

w; UAS-GFP-HNT$_{(III)}$	L. Ming
w; UAS-GFP-HNT^{J27}	Reed Lab Stock Collection
w; sna^{Sco}/CyO ; tubGAL80^{ts}	Bloomington Drosophila Stock Center
w; UAS-GFP-HNT$_{(II)}$; tubGAL80^{ts}	Reed Lab Stock Collection
Act5cGAL4/CyO	Bloomington Drosophila Stock Center
yw GS1018/FM7	Kyoto Drosophila Genetic Resource Center
w; GMR-GAL4	Bloomington Drosophila Stock Center
hnt^{peb} (on X)	Reed Lab Stock Collection
w; Egfr^{f2} /CyO, dp^{lvl}, tub	Bloomington Drosophila Stock Center
UbiDECadherinGFP/CyO	Bloomington Drosophila Stock Center
Lachesin-GFP	Bloomington Drosophila Stock Center
yw;; dronc51/TM6, sb	Bloomington Drosophila Stock Center
w; UAS-Cherry^{NLS}; daGAL4 + DPax2^{B1}GFP/TM6, Tb, Sb	Reed Lab Stock Collection
EP55;; eyeless-218GAL4 / TM6B	Reed Lab Stock Collection

Table A2. Crossing Schemes

Figure #		Crossing Schemes
3.1	3.1D	*w;; daGAL4* × *yw; UAS-N^{intra}/CyO* → *(y)w; N^{intra}/+ ; daGAL4/+*
	3.1F	*w;; daGAL4* × *Df(1)rb^{1}/FM7* → *Df(1)rb^{1}/+;; daGAL4/+* *Df(1)rb^{1}/+;; daGAL4/+* × *yw; UAS-N^{intra}/CyO* → *Df(1)rb^{1}/+; N^{intra}/+; daGAL4/+*
3.2		*w;; daGAL4* × *yw; UAS-N^{intra}/CyO* → *(y)w; N^{intra}/+ ; daGAL4/+*
3.3	3.3F, H	*yw hnt^{XE81}FRT19A/FM7* × *w;; DPax2^{D7}-GFP* → *yw hnt^{XE81}FRT19A /+;; DPax2^{D7}-GFP /+*
	3.3I	*yw; BO-GAL4* × *w; UAS-GFP^{nls14}* → *(y)w; BO-GAL4 /+ ; UAS-GFP^{nls14}/+*
	3.3J	*yw hnt^{XE81}FRT19A/FM7* × *w; UAS-GFP^{nls14}* → *yw hnt^{XE81}FRT19A /+;; UAS-GFP^{nls14}/+* *yw hnt^{XE81}FRT19A /+;; UAS-GFP^{nls14}/+* × *yw; BO-GAL4* → *yw hnt^{XE81}FRT19A /+; BO-GAL4/+ ; UAS-GFP^{nls14}/+*
3.5	3.5A	*w; UbiDECadGFP + Egfr^{1a15}/CyO, TwiG* × *w; Egfr^{f2} /CyO* → *w; UbiDECadGFP + Egfr^{1a15}/ Egfr^{f2}*
	3.5B	*w;; daGAL4* × *w;; UAS-sSpi/TM6 [Gal80]* → *w;; daGAL4/UAS-sSpi*
	3.5C	*w;; daGAL4* × *w;; UAS-Ras85D^{V12}* → *w;; daGAL4/UAS-Ras85D^{V12}*
3.6	3.6B	*w;; daGAL4* × *w; UAS-GFP-HNT$_{(II)}$* → *w; UAS-GFP-HNT$_{(II)}$ /+; daGAL4/+*
	3.6C	Making *daGAL4+DPax2^{B1}dsRed* recombinants: *w;; daGAL4* × *w;; DPax2^{B1}dsRed* → *w;; daGAL4/ DPax2^{B1}dsRed* *w;; daGAL4/ DPax2^{B1}dsRed* × *w; UAS-GFP^{nls14}* → select recombinants: *w; UAS-GFP^{nls14}; daGAL4+ DPax2^{B1}dsRed /+* *w; UAS-GFP^{nls14}; daGAL4+ DPax2^{B1}dsRed /+* × *yw;; dronc51/TM6, sb* → select: *w; +; daGAL4+ DPax2^{B1}dsRed / TM6, sb* *w; +; daGAL4+ DPax2^{B1}dsRed / TM6, sb* × *w; +; daGAL4+ DPax2^{B1}dsRed / TM6, sb* → select: *w;; daGAL4+ DPax2^{B1}dsRed*
		w;; daGAL4+ DPax2^{B1}dsRed × *w; UAS-GFP-HNT$_{(II)}$* → *w; UAS-GFP-HNT$_{(II)}$ /+; daGAL4+ DPax2^{B1}dsRed/+*
3.7	3.7A	*w;; daGAL4* × *Act5cGAL4/CyO*

		→ *w; Act5cGAL4/+; daGAL4/+* *yw EP55 FRT19A ;; DPax2^{B1}dsRed* × *w; Act5cGAL4/+; daGAL4/+* → *yw EP55 FRT19A /+; Act5cGAL4/+; daGAL4/ DPax2^{B1}dsRed*
	3.7B	*w;; daGAL4* × *yw GS1018/FM7* → *yw GS1018/+;; daGAL4/+*
	3.7C	*w;; daGAL4+ DPax2^{B1}dsRed* × *w;; UAS-GFP-HNT$_{(III)}$* → *w;; daGAL4+ DPax2^{B1}dsRed/ UAS-GFP-HNT$_{(III)}$*
3.9	3.9A	*N^{55e11}/FM7c* × *w;; daGAL4* → *N^{55e11}/+;;daGAL4/+* *N^{55e11}/+;;daGAL4/+* × *w; UAS-GFP-HNT$_{(II)}$* → *N^{55e11}/+; UAS-GFP-HNT$_{(II)}$/+;daGAL4/+*
	3.9B	Making *UAS-GFP-HNT$_{(II)}$ + Egfr^{f2}* recombinants: *w; UAS-GFP-HNT$_{(II)}$* × *w; Egfr^{f2} /CyO, dp^{lvl}, tub* → select no CyO: *w; UAS-GFP-HNT$_{(II)}$/ Egfr^{f2}* *w; UAS-GFP-HNT$_{(II)}$/ Egfr^{f2}* × *w; Gla/CyO* → select single males: *w; UAS-GFP-HNT$_{(II)}$(Egfr^{f2})/CyO* *w; dp^{1a15}UbiDECadGFPEgfr^{1a15}/CyO* × *w; UAS-GFP-HNT$_{(II)}$(Egfr^{f2})/CyO* → select lines that throw no Cy+, select virgin female and males: *w; UAS-GFP-HNT$_{(II)}$ + Egfr^{f2}/CyO* × *w; UAS-GFP-HNT$_{(II)}$ + Egfr^{f2}/CyO* → *w; UAS-GFP-HNT$_{(II)}$ + Egfr^{f2}/CyO*
		w; UbiDECadGFP + Egfr^{1a15}/CyO, TwiG × *w;; DPax2^{B1}dsRed* → select no CyO: *w; UbiDECadGFP + Egfr^{1a15}/+; DPax2^{B1}dsRed / +* *w; UbiDECadGFP + Egfr^{1a15}/+; DPax2^{B1}dsRed / +*× *w; UAS-GFP-HNT$_{(II)}$ + Egfr^{f2}/CyO* → *w; UbiDECadGFP + Egfr^{1a15}/ UAS-GFP-HNT$_{(II)}$ + Egfr^{f2} ; DPax2^{B1}dsRed / +*
	3.9C	*w; Egfr^{f2} /CyO* × *w;; DPax2^{B1}dsRed* → select no CyO: *w; Egfr^{f2} /+; DPax2^{B1}dsRed/+* *w; Egfr^{f2} /+; DPax2^{B1}dsRed/+* × *w; UbiDECadGFP + Egfr^{1a15}/CyO, TwiG* → *w; Egfr^{f2} / UbiDECadGFP + Egfr^{1a15}; DPax2^{B1}dsRed/+*
3.10	3.10A	*w; UAS-GFP-HNT$_{(II)}$ + Egfr^{f2}/CyO* × *w;; daGAL4+ DPax2^{B1}dsRed* → *w; UAS-GFP-HNT$_{(II)}$ + Egfr^{f2}/+; DPax2^{B1}dsRed / +*
	3.10B	*UAS-Ras85D^{N17}* × *w; UAS-GFP-HNT$_{(II)}$* → pick males *UAS-Ras85D^{N17}*/Y*; UAS-GFP-HNT$_{(II)}$* *UAS-Ras85D^{N17}* × *UAS-Ras85D^{N17}*/Y*; UAS-GFP-HNT$_{(II)}$* → pick females *UAS-Ras85D^{N1}; UAS-GFP-HNT$_{(II)}$ / +*

		UAS-Ras85D^{N1}; UAS-GFP-HNT$_{(II)}$ / + w;; daGAL4+ DPax2^{B1}dsRed → *UAS-Ras85D^{N1}; UAS-GFP-HNT$_{(II)}$ / +; daGAL4+ DPax2^{B1}dsRed / +*
	3.10C	*w; UAS-Cherry^{NLS}; daGAL4 + DPax2^{B1}GFP/TM6, Tb, Sb × w;; UAS-Ras85D^{V12}* → *w; UAS-Cherry^{NLS}/+; UAS-Ras85D^{V12}/ daGAL4 + DPax2^{B1}GFP*
	3.10D	*w; UAS-Cherry^{NLS}; daGAL4 + DPax2^{B1}GFP/TM6, Tb, Sb × w;; UAS-sSpi/TM6 [Gal80]* → *w; UAS-Cherry^{NLS}/+; UAS-sSpi / daGAL4 + DPax2^{B1}GFP*
	3.10E	*ywEP55;; eyeless-218GAL4 / TM6B × w;; UAS-Ras85D^{V12}* →select and cross vigin females and males no rough eyes: *EP55/(+)(Y);; UAS-Ras85D^{V12}/ TM6B* *EP55;; UAS-Ras85D^{V12}/ TM6B × w; UAS-Cherry^{NLS}; daGAL4 + DPax2^{B1}GFP/TM6, Tb, Sb* → *EP55; UAS-Cherry^{NLS}/+; UAS-Ras85D^{V12}/ daGAL4 + DPax2^{B1}GFP*
3.12	3.12B,C	*Lachesin-GFP × w;; DPax2^{B1}dsRed* → *w;Lachesin-GFP/+; DPax2^{B1}dsRed/+*
3.13	3.13A-D	*w; GMR-GAL4 × w;; DPax2^{B1}dsRed* → *w; GMR-GAL4/+ ; DPax2^{B1}dsRed/+* *w; GMR-GAL4/+ ; DPax2^{B1}dsRed/+ × w; UAS-GFP-HNT$_{(II)}$*; tubGAL80^{ts} → grow at 18° until 24 hr APF, shift to 29° for 24 hrs *w; GMR-GAL4/ UAS-GFP-HNT$_{(II)}$; DPax2^{B1}dsRed/*tubGAL80^{ts}
3.14	3.14 A,D	*w; GMR-GAL4 × w;; DPax2^{B1}dsRed* → *w; GMR-GAL4/+ ; DPax2^{B1}dsRed/+* *w; GMR-GAL4/+ ; DPax2^{B1}dsRed/+ × w;; UAS-GFP-HNT^{J27}* → *w; GMR-GAL4/+ ; DPax2^{B1}dsRed/ UAS-GFP-HNT^{J27}*
	3.14 C	*w; GMR-GAL4 × w;; DPax2^{B1}dsRed* → *w; GMR-GAL4/+ ; DPax2^{B1}dsRed/+* *UbiDECadherinGFP/CyO × w;; UAS-GFP-HNT^{J27}* →*w; UbiDECadherinGFP/+; UAS-GFP-HNT^{J27}* *w; GMR-GAL4/+ ; DPax2^{B1}dsRed/+ × w; UbiDECadherinGFP/+; UAS-GFP-HNT^{J27}* → *w; GMR-GAL4/ UbiDECadherinGFP ; DPax2^{B1}dsRed/ UAS-GFP-HNT^{J27}*

Appendix B: Characterization of DPax2 reporter lines

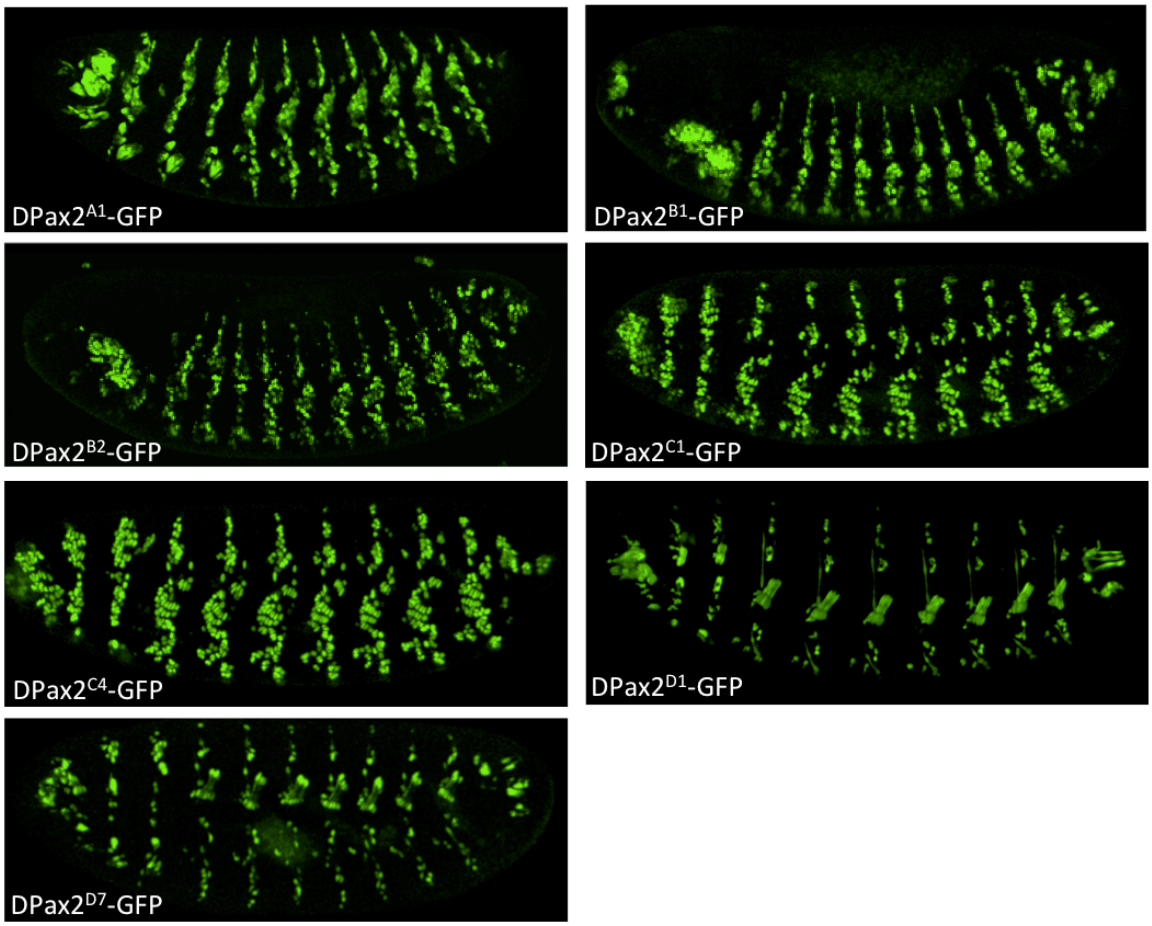

Figure A1 Characterization of different DPax2 reporter lines constituted from fragments of the large *sv* enhancer

All DPax2 reporter lines, constructed and provided to us by Dr. Joshua Kavaler, show differential expression. All of the above reporter lines were constructed using fragments of the large *sv* enhancer as described by (Johnson et al., 2011).